

An Energy-Aware Retransmission Approach in SWIPT-Based Cognitive Relay Systems

Qiang Li¹, Member, IEEE, Xueyan Zhang, Ashish Pandharipande, Senior Member, IEEE, Xiaohu Ge², Senior Member, IEEE, and Hamid Gharavi, Life Fellow, IEEE

Abstract—In this paper, cooperative spectrum sharing is considered between a primary user (PU) and a secondary user (SU), where the off-the-grid secondary transmitter (ST) serves as a cognitive relay to forward both the received primary and secondary signals by exploiting simultaneous wireless information and power transfer (SWIPT). Based on a two-phase relaying model, power splitting is adopted by the ST for energy harvesting and information processing in the first phase. Next, the harvested energy at the ST is used to amplify-and-forward a linearly weighted combination of the primary and secondary signals, in the second phase. To enhance the reliability of the system and utilize the energy harvested more wisely, an energy-aware retransmission (EAR) scheme is proposed in the first phase to guarantee that a certain minimum amount of energy is collected by the ST before launching the second phase. Both outage and throughput performances are theoretically analyzed for the PU and the SU. Simulation results demonstrate that a win-win relationship is built between the PU and the SU under proper parameter configurations, and the proposed EAR scheme can bring additional performance gains in unfavorable conditions imposed under *high rate and low power*.

Index Terms—Cooperative spectrum sharing, cognitive relay, simultaneous wireless information and power transfer, power splitting, energy-aware retransmission.

I. INTRODUCTION

TRADITIONAL options to prolong the lifetime of energy-constrained wireless networks using rechargeable, replaceable batteries are inconvenient or even unusable in certain applications [1]. An alternative approach is to scavenge energy from the surrounding environment, e.g., energy harvesting (EH) from the solar, wind, and radio-frequency (RF) signal radiations [2]. This option, in theory, has the potential to provide unlimited power supply to wireless devices, e.g., sensors, without consuming extra fossil fuels [3], [4]. Due to

the highly dynamic operating environment, however, there is a great uncertainty in the amount of energy harvested. In order to provide a stable power supply for the sustainable operation of wireless networks, dedicated RF transmitters or wireless power beacons have been proposed to achieve efficient wireless power transfer [5]–[8]. By creating a twofold tunnel for transferring both information and energy [9], the RF signals enable simultaneous wireless information and power transfer (SWIPT), which significantly improves the efficiency of energy-constrained wireless networks [10]–[14].

In addition to linear EH models [8]–[10], a parametric non-linear EH model is also proposed in [15], which is capable of achieving better accuracy for practical EH circuits. Based on this model, various resource allocation strategies are then proposed for systems with a single antenna [16], multiple antennas [17], [18], and for cognitive wireless-powered communication networks [19], [20], respectively. Further improvements have also been reported for SWIPT-based MIMO broadcasting systems [21] and energy-constrained relaying networks [22] under power-splitting and time-switching paradigms.

Given that the spectrum and energy efficiencies are amongst the most essential design metrics in wireless communications systems, there has been an increasing interest in applying SWIPT to cognitive radios for enhancing both the spectrum and energy efficiencies of wireless networks. For a *detect-and-avoid* paradigm [23] where an EH-based secondary user (SU) opportunistically accesses the spectrum holes to avoid interfering the legacy primary user (PU), various spectrum access policies [24]–[26] are proposed for enhancing the achievable system throughput [27]–[29]. For a *harvest-then-transmit* paradigm [30], the SU implicitly harvests the RF energy by overhearing the PU transmission over a number of successive time blocks without interrupting the primary link, and the spectrum sharing begins when the ST has harvested enough energy. For an *interference temperature* paradigm [23] where the SU is allowed to access the licensed spectrum simultaneously with the PU, the off-the-grid SU has to rely on the energy harvested from the RF radiations of PU and strictly control its transmission power to maintain a certain interference or outage constraint at the PU [31]–[33]. A resource complementary scenario is considered in [34] based on a *spectrum leasing* concept [35]. Using this approach the SU exploits its energy transfer and relay functions to enable earlier completion of the PU's transmission [36], in exchange for some dedicated spectra to transmit the secondary signals

Manuscript received November 12, 2018; revised March 8, 2019; accepted April 8, 2019. Date of publication April 16, 2019; date of current version September 9, 2019. The authors would like to acknowledge the support from National Key R&D Program of China (2016YFE0133000); EU-China study on IoT and 5G (EXCITING-723227). The associate editor coordinating the review of this paper and approving it for publication was D. Niyato. (Corresponding author: Xiaohu Ge.)

Q. Li, X. Zhang, and X. Ge are with the School of Electronic Information and Communications, Huazhong University of Science and Technology, Wuhan 430074, China (e-mail: qli_patrick@hust.edu.cn; xueyazhang@hust.edu.cn; xhge@hust.edu.cn).

A. Pandharipande is with Signify, 5656 AE Eindhoven, The Netherlands (e-mail: ashish.p@signify.com).

H. Gharavi is with the National Institute of Standards and Technology, Gaithersburg, MD 20899 USA (e-mail: hamid.gharavi@nist.gov).

Digital Object Identifier 10.1109/TCCN.2019.2911680

exclusively. Furthermore, EH via SWIPT has also been applied to a cognitive *overlay* paradigm [23] where an SU in the same frequency band can send its own signal along with the received primary signal (functioning as a relay) using amplify-and-forward (AF) [37], [38] or decoded-and-forward (DF) [39], [40]. A wireless energy harvesting and information transfer protocol is investigated in [37], [38] for cognitive relay networks, where a secondary network shares the spectrum while harvesting energy by assisting the primary transmission. The exact expression of outage probability and rate-energy tradeoff has also been analyzed in [37], [38]. Three-phase energy harvesting and information transmission protocol is proposed in [41] for cognitive radio sensor networks, where the energy-constrained secondary sensors serve as DF relay nodes to forward the primary information with the purpose of accessing the licensed spectrum. This includes an optimal relay selection algorithm for maximizing the ergodic throughput of primary users.

In order to enhance the spectrum utilization of wireless networks while solving the limitations imposed by energy-constrained wireless devices, in this paper we investigate a cooperative spectrum sharing system assisted by an SWIPT-based cognitive relay. The PU, consisting of a primary transmitter-receiver (PT-PR) pair, owns the spectrum but has a very weak direct channel from PT→PR. On the other hand, the SU, consisting of a secondary transmitter-receiver (ST-SR) pair, is located in between the PT and the PR, thus has a better channel from/to the PT/PR. Then the off-the-grid ST, instead of waiting for an opportunistic access, will be allowed to act as a cooperative relay to improve the performance of PU by using the harvested energy scavenged from the RF radiations of the PT. In return, the secondary signal is superimposed on the primary signal and forwarded simultaneously by the ST, subject to a certain power allocation. The main contributions of this work are summarized as follows:

- A two-phase AF relaying model is established for a cooperative spectrum sharing system assisted by a SWIPT-based cognitive relay ST involving two co-existing systems and many parameters. In the first phase, power splitting is employed at the ST where the received signal from PT is divided into two parts for information processing and EH. The harvested energy is then used to forward a linearly weighted combination of the primary signal and secondary signal with a certain power allocation, in the second phase. Unlike in [9] and [38], where the direct channel between PT and PR has been ignored, in our work the signals received through both the relay channel PT→ST→PR and the direct channel PT→PR (albeit weak) are utilized for decoding at the PR. This makes it more challenging to analyze the end-to-end performance of PU.
- A baseline scheme with a single transmission in the first phase is first analyzed, where the energy harvested by the ST, no matter how much, is directly used to power the relaying transmission. This may result in a high outage probability due to limited energy availability, subsequently causing unnecessary energy wastage. To enhance system reliability while using the harvested energy more

wisely, an energy-aware retransmission (EAR) scheme is proposed. In this approach, the PT performs retransmissions within a permitted number of retransmissions in the hope that a certain minimum amount of energy (i.e., based on the energy threshold) is harvested by the ST before launching the subsequent relaying transmission. It requires sophisticated definitions and characterizations of different cases across multiple time slots, which makes the analysis very challenging.

- The outage probability and throughput are analytically derived for both the PU and the SU. Based on our analytical results, we are able to accurately evaluate throughput performances of the whole SNR regime under various channel and rate conditions. Simulation results demonstrate that when the PU suffers from severe path-loss attenuations, the SU is allowed to access the licensed spectrum and at the same time performance gains are achieved for the PU as compared with the case without spectrum sharing, hence resulting in a win-win situation between the PU and the SU. Furthermore, with a proper selection of the energy threshold for EH and the retransmission threshold, the energy harvested over retransmissions can be exploited by the proposed EAR scheme wisely, which shows additional performance gains over the baseline scheme and the case without spectrum sharing under *high rate* and *low power* conditions.

Although retransmission policies have been proposed for point-to-point dual EH links [42] and multiple EH-based DF relays [43] recently, the focus is on power management for minimizing the packet drop probability. By contrast, an SWIPT-based cooperative spectrum sharing system is focused, where both outage and throughput performances of the system can be enhanced by the proposed EAR scheme with proper selections of the thresholds for energy and retransmission.

II. SYSTEM MODEL

As shown in Fig. 1(a), we consider a cognitive spectrum sharing system where an ST-SR pair wishes to access the spectrum licensed to a PT-PR pair and all terminals operate in half-duplex mode. The PT is connected to a stable power supply and transmits signal x_p at a fixed power P_p . The off-the-grid ST relies on the energy harvested from the RF radiations of the PT to remain active in the network and transmits with best-effort at a power P_s that is a random variable depending on the harvested energy. Denote $h_{p,p}$, $h_{p,s}$, $h_{p,r}$, $h_{s,p}$, and $h_{s,r}$ as the corresponding coefficients of channels PT→PR, PT→ST, PT→SR, ST→PR, and ST→SR, respectively. Although SWIPT typically relies on line-of-sight (LoS) links to overcome severe power attenuation, in urban environments a perfect LoS links may not be guaranteed due to the rich scatters/reflectors or obstacles moving into the SWIPT path. As such, we adopt a Rayleigh fading model by taking into account the path-loss attenuations [9], [14]. Then we have the channel coefficient $h_{j,k} \sim \mathcal{CN}(0, d_{j,k}^{-\nu})$, where $j \in \{p, s\}$ and $k \in \{p, s, r\}$, $d_{j,k}$ denotes the corresponding distance between j and k , and ν denotes the path-loss exponent. Denoting $\gamma_{j,k} = |h_{j,k}|^2$ as the channel power gain, we have

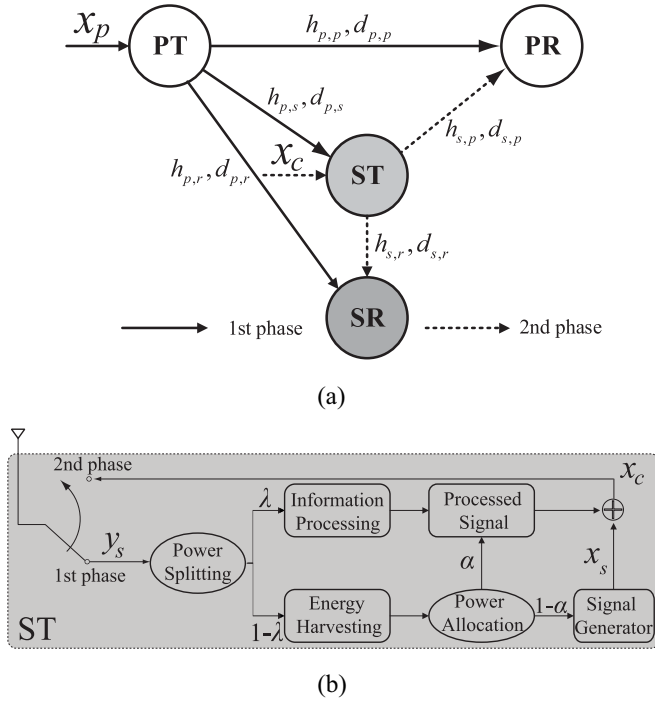


Fig. 1. Illustrations of the system model on a two-phase AF relaying protocol. (a) The considered cooperative spectrum sharing system in which the SWIPT-based ST serves as the cognitive relay. (b) A two-phase relaying protocol with power splitting performed at ST for EH and information processing respectively.

$\gamma_{j,k} \sim \exp(d_{j,k}^\nu)$. The additive white Gaussian noise (AWGN) at the respective receivers is denoted by $n_k \sim \mathcal{CN}(0, \sigma^2)$, $k \in p, s, r$.

Provided the dense urban environmental conditions, it is assumed that the direct channel PT→PR suffers from severe path-loss attenuations due to obstacles or deep fading [14], [44], [45]. Then the PU has to rely on close-by terminals that provide cooperative relaying transmissions. An ST that is located in between the PT and the PR, having a better channel and signal observation from (to) the PT (PR), is willing to serve as a cognitive relay for the primary system in exchange for spectrum access opportunities. Then, through a series of well-defined handshake operations [23], the cooperative spectrum sharing can be established between the PT-ST pair and the ST-SR pair by exploiting the cognitive and cooperative relaying transmission provided by the ST. To be specific, an AF relaying protocol [9] is considered and the transmission of a primary signal x_p (and secondary signal x_s) can be divided into two successive phases, as illustrated in Fig. 1(b).

- In the first phase, the PT transmits a primary signal x_p to the ST where SWIPT is performed. To be specific, the corresponding received signal observation at the ST is split into two portions for information processing and EH respectively, with a power splitting factor λ [46]. The energy harvested is then stored in a battery of sufficiently large capacity [47].
- In the second phase, the ST transmits the locally generated secondary signal x_s along with x_p after amplification to a certain power constraint. To be specific, a composite signal x_c that is a linearly weighted sum of the primary

and secondary signals is transmitted by ST by using the harvested energy, subject to a certain power allocation factor α between them.

Since x_p and x_s are transmitted simultaneously by the ST in the second phase, spectrum sharing can be achieved simultaneously between the PU and the SU in the same frequency band, which significantly improves system spectrum efficiency without consuming extra energy. Note that the interference brought to PU due to the transmission of x_s can be potentially compensated by selecting a suitable power allocation factor α [48], [49], as will be shown later in Section V.

III. A BASELINE SCHEME WITH A SINGLE TRANSMISSION

Based on the system model introduced in Section II, we first consider a baseline scheme with a single transmission in the first phase. As shown in Fig. 2(a), slot-based transmissions are considered where each phase consists of a single time slot. Since only a small fraction of each time slot can be occupied for control signaling exchanges (e.g., pilot sequence for channel estimation), its interval is very short compared to the duration of data transmission and therefore can be ignored [9], [34], [38]. Thus, it is assumed that the effective communication time equals the duration in each time slot.

In the first phase, the PT transmits a signal x_p at a predefined target rate R_p . Then the corresponding received signal at the PR, ST, and SR is given as

$$y_k = \sqrt{P_p} h_{p,k} x_p + n_k, \quad k \in \{p, s, r\}. \quad (1)$$

As illustrated in Fig. 1(b), power splitting [12] is performed at the ST where a fraction λ of the received signal observation y_s is used for information forwarding, with the remaining $\bar{\lambda} = 1 - \lambda$ for EH [46]. In general, estimating the optimal power splitting factor, in terms of end-to-end system performance, would require the instantaneous availability of the perfect global channel state information, which cannot be practically obtained at the intermediate relay ST. Thus, we select a fixed power splitting factor that can achieve a reasonably good performance on average [22], [38]. Assuming that the energy consumed in receiving and processing signal is negligible, a pessimistic case is considered where the power splitting only acts on the signal and not on the noise power. Then the energy harvested by the ST at the end of the first phase is given by

$$E_h = \eta \bar{\lambda} P_p |h_{p,s}|^2, \quad (2)$$

where $\eta \in (0, 1)$ denotes the energy conversion efficiency.

In the second phase, with a power allocation factor α between x_p and x_s , a composite signal

$$x_c = \sqrt{\alpha P_s} \beta (\sqrt{\lambda} y_s + n_0) + \sqrt{(1-\alpha) P_s} x_s \quad (3)$$

is transmitted by the ST with best-effort, i.e., all energy harvested in (2) is used for transmission where $P_s = \eta \bar{\lambda} P_p |h_{p,s}|^2$. Here $n_0 \sim \mathcal{CN}(0, \sigma_0^2)$ denotes the noise introduced by signal conversion from bandpass to baseband, and

$$\beta = \frac{1}{\sqrt{\lambda P_p |h_{p,s}|^2 + \lambda \sigma^2 + \sigma_0^2}} \approx \frac{1}{\sqrt{\lambda P_p |h_{p,s}|^2}} \quad (4)$$

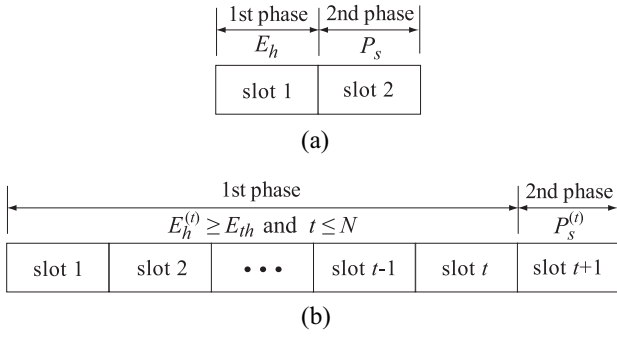


Fig. 2. A slot-based two-phase model, where E_h represents the energy harvested by ST after a single transmission in (2), and $E_h^{(t)}$, E_{th} , and N represent the energy harvested by ST after t transmissions in (18), the energy threshold for EH, and the retransmission threshold, respectively. (a) A baseline scheme with a single transmission in the first phase. (b) Proposed EAR scheme with retransmissions in the first phase.

denotes the power amplification factor obtained assuming $P_p \gg \sigma^2, \sigma_0^2$ [49]. Then, the corresponding received signal at the PR and the SR at the end of the second phase is given as

$$\begin{aligned} y_k &= h_{s,k}x_c + n_k, \quad k \in \{p, r\} \\ &= \beta\sqrt{\alpha\lambda P_s P_p} h_{p,s} h_{s,k} x_p + \sqrt{(1-\alpha)P_s} h_{s,k} x_s \\ &\quad + \beta\sqrt{\alpha\lambda P_s} h_{s,k} n_s + \beta\sqrt{\alpha P_s} h_{s,k} n_0 + n_k. \end{aligned} \quad (5)$$

A. Outage Analysis of Primary System

By maximal-ratio combining (MRC) of the received signals (1) and (5) through both the direct and the relay channels in two successive phases, the received signal-to-interference-plus-noise ratio (SINR) at the PR is expressed as

$$\begin{aligned} \gamma_p &= \frac{P_p |h_{p,p}|^2}{\sigma^2} \\ &\quad + \frac{\beta^2 \alpha \lambda P_s P_p |h_{p,s}|^2 |h_{s,p}|^2}{(1-\alpha)P_s |h_{s,p}|^2 + \beta^2 \alpha P_s |h_{s,p}|^2 (\lambda \sigma^2 + \sigma_0^2) + \sigma^2} \\ &\approx \frac{P_p |h_{p,p}|^2}{\sigma^2} + \frac{P_p \xi_1 |h_{p,s}|^2 |h_{s,p}|^2}{(P_p \xi_2 |h_{p,s}|^2 + \xi_1 \varphi) |h_{s,p}|^2 + \sigma^2} \end{aligned} \quad (6)$$

$$\approx \frac{P_p |h_{p,p}|^2}{\sigma^2} + \frac{P_p \xi_1 |h_{p,s}|^2 |h_{s,p}|^2}{P_p \xi_2 |h_{p,s}|^2 |h_{s,p}|^2 + \sigma^2}, \quad (7)$$

where $\xi_1 = \alpha \eta \bar{\lambda}$, $\xi_2 = (1-\alpha) \eta \bar{\lambda}$, and $\varphi = \sigma^2 + \frac{\sigma_0^2}{\lambda}$. The approximation in (6) is obtained from (4), and the approximation in (7) is obtained assuming $\xi_1 \varphi |h_{s,p}|^2 \ll \sigma^2$. For a general network topology where nodes are located relatively apart from each other, this would be a reasonable assumption and, for most cases, we have $|h_{s,p}|^2 \ll 1$ as the result of path-loss attenuations.

Here, we adopt an outage definition that is widely used in systems with retransmissions [50]–[52], where the outage probability characterizes how reliably a message can be eventually delivered, irrespective of the number of occupied time slots. Defining $\gamma_{p,0} = 2^{R_p} - 1$ as the SINR threshold for successfully decoding x_p , the outage probability for the primary system can then be expressed as

$$O_p = \Pr\{\log_2(1 + \gamma_p) < R_p\} = \Pr\{\gamma_p < \gamma_{p,0}\}, \quad (8)$$

which is theoretically analyzed and summarized in Theorem 1.

Theorem 1: For the considered baseline scheme, the PT performs a single transmission in the first phase and the ST uses the harvested energy to transmit a linearly weighted sum of the primary and secondary signals in the second phase. Denoting $x = |h_{p,s}|^2$, $y = |h_{s,p}|^2$ and $z = |h_{p,p}|^2$, the end-to-end outage probability of the PU can be obtained as

$$\begin{cases} 1 - d_{p,s}^v e^{d_{p,p}^v \left(\frac{\xi_1 \sigma^2}{P_p \xi_2} - \frac{\gamma_{p,0} \sigma^2}{P_p} \right)} \int_0^\infty I_1(x) dx, \\ \text{when } 0 < \alpha \leq \frac{\gamma_{p,0}}{1 + \gamma_{p,0}}, \\ 1 - 2 \sqrt{\frac{d_{p,s}^v d_{s,p}^v \gamma_{p,0} \sigma^2}{\phi_1}} K_1 \left(2 \sqrt{\frac{d_{p,s}^v d_{s,p}^v \gamma_{p,0} \sigma^2}{\phi_1}} \right) \\ - d_{p,s}^v e^{d_{p,p}^v \left(\frac{\xi_1 \sigma^2}{P_p \xi_2} - \frac{\gamma_{p,0} \sigma^2}{P_p} \right)} \int_0^\infty [I_1(x) - I_2(x)] dx, \\ \text{when } \frac{\gamma_{p,0}}{1 + \gamma_{p,0}} < \alpha < 1, \end{cases} \quad (9)$$

where $\phi_1 = P_p(\xi_1 - \xi_2 \gamma_{p,0})$, $I_1(x) = e^{-d_{p,s}^v x + \frac{d_{s,p}^v \sigma^2}{P_p \xi_2 x}} \Gamma(1, \frac{d_{s,p}^v \sigma^2}{P_p \xi_2 x}; \frac{d_{s,p}^v \xi_1 \sigma^4}{P_p^2 \xi_2^2 x})$, $I_2(x) = e^{-d_{p,s}^v x + \frac{d_{s,p}^v \sigma^2}{P_p \xi_2 x}} \Gamma(1, \frac{d_{s,p}^v \sigma^2}{P_p \xi_2 x} + \frac{d_{s,p}^v \gamma_{p,0} \sigma^2}{\phi_1 x}; \frac{d_{s,p}^v \xi_1 \sigma^4}{P_p^2 \xi_2^2 x})$, $K_v(\cdot)$ denotes the modified Bessel function of the second kind with order v [53], and $\Gamma(a, x; b)$ is the generalized incomplete Gamma function defined by $\Gamma(a, x; b) \triangleq \int_x^\infty t^{a-1} e^{-(t-\frac{b}{t})} dt$ [54].

Proof: See Appendix A. \blacksquare

B. Outage Analysis of Secondary System

By using conventional training sequences, the corresponding channel state information of the incoming channel PT \rightarrow SR can be estimated accurately at the receiver side SR [38], [55], [56] for information detection. Since the focus of our work is on the performance analysis of the proposed EAR scheme over multiple time slots, an upper bound performance is considered for the secondary system. Under these conditions, the SR can correctly decode the primary signal x_p in the first phase [38], [48]. Then, the interference component of x_p , after being reconstructed using the estimated channel state information, is removed from the received signal at SR in the second phase leading to a perfect interference cancellation of the PU signal [38], [39]. Then from (5), the effectively received signal at the SR is given as

$$\begin{aligned} y_r' &= \sqrt{(1-\alpha)P_s} h_{s,r} x_s + \beta\sqrt{\alpha\lambda P_s} h_{s,r} n_s \\ &\quad + \beta\sqrt{\alpha P_s} h_{s,r} n_0 + n_r. \end{aligned} \quad (10)$$

The corresponding received signal-to-noise ratio (SNR) at the SR is expressed as

$$\begin{aligned} \gamma_s &= \frac{(1-\alpha)P_s |h_{s,r}|^2}{\beta^2 \alpha P_s |h_{s,r}|^2 (\lambda \sigma^2 + \sigma_0^2) + \sigma^2} \\ &\approx \frac{P_p \xi_2 |h_{p,s}|^2 |h_{s,r}|^2}{\xi_1 \varphi |h_{s,r}|^2 + \sigma^2} \end{aligned} \quad (11)$$

$$\approx \frac{P_p \xi_2 |h_{p,s}|^2 |h_{s,r}|^2}{\sigma^2}. \quad (12)$$

Similarly, the approximation in (11) is obtained from (4), and the approximation in (12) is obtained assuming $\xi_1 \varphi |h_{s,r}|^2 \ll \sigma^2$. Defining $\gamma_{s,0} = 2^{R_s} - 1$ as the SNR threshold for successfully decoding x_s where R_s denotes the target rate of x_s , then an outage occurs for the SU with a probability

$$O_s = \Pr\{\gamma_s < \gamma_{s,0}\}, \quad (13)$$

as theoretically analyzed and summarized in Theorem 2.

Theorem 2: For the considered baseline scheme, by letting $x = |h_{p,s}|^2$, $y = |h_{s,r}|^2$ and $\phi_2 = \frac{d_{p,s}^v d_{s,r}^v \gamma_{s,0} \sigma^2}{P_p \xi_2}$, the outage probability of the SU can be obtained as

$$O_s = 1 - 2\sqrt{\phi_2} K_1 \left(2\sqrt{\phi_2} \right). \quad (14)$$

Proof: See Appendix B. ■

C. Throughput Analysis

As shown in Fig. 2(a), since each phase consists of a single time slot, the average throughput, which is defined as the total amount of data successfully received by the PU (or SU) per time slot [27], can be expressed as

$$T_p = \frac{(1 - O_p)R_p}{2}, \quad (15)$$

$$T_s = \frac{(1 - O_s)R_s}{2}. \quad (16)$$

IV. PROPOSED EAR SCHEME

For the above baseline scheme where the PT performs only a single transmission in the first phase, it is assumed that the energy harvested E_h , no matter how much, can be directly used to power the transmission in the second phase [38]–[40], [46]. This may not be the case in practical systems where a certain minimum amount of energy, e.g., circuit power consumption, is required before a transmission can take place [47]. Additionally, the energy harvested after a single transmission may not be sufficient to enable successful delivery of x_p and x_s in the second phase, leading to a high outage probability and energy wastage. In order to enhance reliability of the system while using the harvested energy more wisely, we propose an EAR scheme.

A. Proposed EAR Scheme With Energy Accumulation in Phase 1

As shown in Fig. 2(b), the PT performs retransmissions of x_p in the first phase until either the energy threshold E_{th} or the retransmission threshold N is firstly hit. Considering that channels keep changing from slot to slot, it is difficult to obtain an accurate instantaneous channel state information of ST→PR at the ST. Thus, rather than adaptively changing the value of E_{th} based on the channel fluctuation for successful transmissions from ST to PR, we assume a fixed value of E_{th} at ST in the hope that statistically a certain outage probability can be achieved at the PR [55], [57]. For simplicity, it is assumed that the feedback of acknowledgement (ACK) or negative acknowledgement (NACK), indicating whether E_{th} is met or not, is error-free and completed immediately with negligible overhead [58]. Then, the corresponding received signal at the PR

and the ST in the t th time slot, where $t \in \{1, \dots, N\}$, can be expressed as

$$y_k(t) = \sqrt{P_p} h_{p,k}(t) x_p + n_k(t), \quad k \in \{p, s\}. \quad (17)$$

Upon power splitting of the received signal observation $y_s(t)$, the energy harvested by the ST up to the t th time slot is given as

$$E_h^{(t)} = \sum_{i=1}^t \eta \bar{\lambda} P_p |h_{p,s}(i)|^2. \quad (18)$$

Depending on when E_{th} is met, we have the following mutually exclusive events.

- $\mathcal{E}_1 = \{\text{The ST harvests sufficient energy after the first time slot, i.e., } E_h^{(1)} \geq E_{th}\}$;
- $\mathcal{E}_2 = \{\bigcup_{t=2}^N \mathcal{E}_2^{(t)} \mid \mathcal{E}_2^{(t)}: \text{The ST harvests sufficient energy right after the } t\text{th time slot, i.e., } E_h^{(t-1)} < E_{th} \leq E_h^{(t)}\}$;
- $\mathcal{E}_3 = \{\text{The ST harvests insufficient energy after } N \text{ time slots, i.e., } E_h^{(N)} < E_{th}\}$.

Remark 1: With a proper selection of the energy threshold, E_{th} , and the retransmission threshold N , a reasonable amount of energy can be accumulated at the ST for enabling a successful delivery of information and without any significant delay. This translates into throughput gains of the proposed EAR scheme, especially in high rate and low power regimes, as will be shown later in Section V. More specifically, when both the baseline scheme and the case without spectrum sharing are stuck in outage due to a very limited energy availability at the ST, it is still possible for the proposed EAR scheme to successfully deliver some information.

For events \mathcal{E}_1 and \mathcal{E}_2 that sufficient energy is harvested at the end of the t th time slot, for $t \in \{1, \dots, N\}$, the ST proceeds to transmit a composite signal

$$x_c = \sqrt{\alpha P_s^{(t)}} \beta \left(\sqrt{\lambda} y_s(t) + n_0 \right) + \sqrt{(1 - \alpha) P_s^{(t)}} x_s \quad (19)$$

in the second phase, where $P_s^{(t)} = \sum_{i=1}^t \eta \bar{\lambda} P_p |h_{p,s}(i)|^2$ and the power amplification factor

$$\beta = \frac{1}{\sqrt{\lambda P_p |h_{p,s}(t)|^2 + \lambda \sigma^2 + \sigma_0^2}} \approx \frac{1}{\sqrt{\lambda P_p |h_{p,s}(t)|^2}} \quad (20)$$

assuming $P_p \gg \sigma^2, \sigma_0^2$. Upon collecting sufficient energy right after the t th time slot, only the latest received signal observation $y_s(t)$ is amplified and forwarded by the ST, as given in (19). Then the corresponding received signal at the PR and the SR in the second phase is given as

$$\begin{aligned} y_k &= h_{s,k} x_c + n_k, \quad k \in \{p, r\} \\ &= \beta \sqrt{\alpha \lambda P_s^{(t)}} P_p h_{p,s}(t) h_{s,k} x_p + \sqrt{(1 - \alpha) P_s^{(t)}} h_{s,k} x_s \\ &\quad + \beta \sqrt{\alpha P_s^{(t)}} h_{s,k} \left(\sqrt{\lambda} n_s + n_0 \right) + n_k. \end{aligned} \quad (21)$$

By MRC of the received signals in (17) and (21) through both the direct and the relay channels in two successive phases, the corresponding received SINR at the PR is given as (22) shown

$$\gamma_p^{(t)} \approx \sum_{i=1}^t \frac{P_p |h_{p,p}(i)|^2}{\sigma^2} + \frac{\alpha \sum_{i=1}^t \eta \bar{\lambda} P_p |h_{p,s}(i)|^2 |h_{s,p}|^2}{(1-\alpha) \sum_{i=1}^t \eta \bar{\lambda} P_p |h_{p,s}(i)|^2 |h_{s,p}|^2 + \sigma^2 + \frac{\alpha \sum_{i=1}^t \eta \bar{\lambda} |h_{p,s}(i)|^2 |h_{s,p}|^2 (\sigma_0^2 + \lambda \sigma^2)}{\lambda |h_{p,s}(t)|^2}} \quad (22)$$

$$\begin{aligned} &= \sum_{i=1}^t \frac{P_p |h_{p,p}(i)|^2}{\sigma^2} + \frac{P_p \xi_1 \sum_{i=1}^t |h_{p,s}(i)|^2 |h_{s,p}|^2}{P_p \xi_2 \sum_{i=1}^t |h_{p,s}(i)|^2 |h_{s,p}|^2 + \frac{\xi_1 \varphi \sum_{i=1}^t |h_{p,s}(i)|^2 |h_{s,p}|^2}{|h_{p,s}(t)|^2} + \sigma^2} \\ &\approx \sum_{i=1}^t \frac{P_p |h_{p,p}(i)|^2}{\sigma^2} + \frac{P_p \xi_1 \sum_{i=1}^t |h_{p,s}(i)|^2 |h_{s,p}|^2}{P_p \xi_2 \sum_{i=1}^t |h_{p,s}(i)|^2 |h_{s,p}|^2 + \sigma^2} \end{aligned} \quad (23)$$

at the top of this page, with the corresponding received SNR at the SR

$$\gamma_s^{(t)} \approx \frac{(1-\alpha) \sum_{i=1}^t \eta \bar{\lambda} P_p |h_{p,s}(i)|^2 |h_{s,r}|^2}{\frac{\alpha \sum_{i=1}^t \eta \bar{\lambda} |h_{p,s}(i)|^2 |h_{s,r}|^2 (\sigma_0^2 + \lambda \sigma_{ps}^2)}{\lambda |h_{p,s}(t)|^2} + \sigma^2} \quad (24)$$

$$\begin{aligned} &= \frac{P_p \xi_2 \sum_{i=1}^t |h_{p,s}(i)|^2 |h_{s,r}|^2}{\frac{\xi_1 \varphi \sum_{i=1}^t |h_{p,s}(i)|^2 |h_{s,r}|^2}{|h_{p,s}(t)|^2} + \sigma^2} \\ &\approx \frac{P_p \xi_2 \sum_{i=1}^t |h_{p,s}(i)|^2 |h_{s,r}|^2}{\sigma^2}. \end{aligned} \quad (25)$$

Similarly, the approximations in (22) and (24) are obtained from (20), and the approximations in (23), as shown at the top of this page and (25) are obtained assuming $\xi_1 \varphi |h_{s,p}|^2 \ll \sigma^2$ and $\xi_1 \varphi |h_{s,r}|^2 \ll \sigma^2$, respectively.

For event \mathcal{E}_3 where an energy outage occurs, i.e., $E_h^{(N)} < E_{th}$, although it would be helpful to consume all the harvested energy at the ST for forwarding x_c in the second phase, we assume that the ST remains silent for the sake of protocol consistency. Then PR attempts to recover x_p by MRC of the received signals through only the direct channel PT→PR across the past N time slots, i.e., $y_p(1), \dots, y_p(N)$. The corresponding received SNR at the PR is expressed as

$$\gamma_d = \sum_{i=1}^N \frac{P_p |h_{p,p}(i)|^2}{\sigma^2}. \quad (26)$$

Remark 2: Conditioned on event \mathcal{E}_3 , although the ST has no chance to transmit in the subsequent relaying phase, the energy harvested $E_h^{(N)}$ can potentially be retained for a future usage. However, since our focus is on the performance analysis for the transmission of a primary message over two successive phases, this scenario is beyond the scope of our manuscript and will be delegated to future works. For tractable analysis, it is assumed that the harvested energy will gradually drain off at the beginning of the transmission of a new primary signal, which could be hours, days or even weeks apart depending on the specific application [56]. This is a reasonable assumption in sensor networks where the low-power sensor node stores the harvested energy in supercapacitors that have the advantages of high energy density, fast charging cycle, and years of charging

and discharging cycles [59], but come at a cost of high self-discharging [60].

B. Outage Analysis of Primary System

With a joint consideration of all possible events in the first phase, the end-to-end outage probability of the primary system under the EAR scheme is derived in Theorem 3.

Theorem 3: For the proposed EAR scheme, taking into account of all possible events \mathcal{E}_1 , \mathcal{E}_2 and \mathcal{E}_3 in the first phase, the overall end-to-end outage probability of PU can be obtained as

$$\begin{aligned} O_p &= \Pr \left\{ \underbrace{\mathcal{E}_1 \cap \left\{ \gamma_p^{(1)} < \gamma_{p,0} \right\}}_{\mathcal{E}_{1,out}} \right\} \\ &\quad + \sum_{t=2}^N \Pr \left\{ \underbrace{\mathcal{E}_2^{(t)} \cap \left\{ \gamma_p^{(t)} < \gamma_{p,0} \right\}}_{\mathcal{E}_{2,out}^{(t)}} \right\} \\ &\quad + \Pr \left\{ \underbrace{\mathcal{E}_3 \cap \left\{ \gamma_d < \gamma_{p,0} \right\}}_{\mathcal{E}_{3,out}} \right\}. \end{aligned} \quad (27)$$

Proof: The probabilities $\Pr\{\mathcal{E}_{1,out}\}$, $\Pr\{\mathcal{E}_{2,out}^{(t)}\}$ and $\Pr\{\mathcal{E}_{3,out}\}$ are derived in *Lemma 1*, *Lemma 2* and *Lemma 3* respectively. ■

Lemma 1: For event $\mathcal{E}_{1,out}$ that the energy harvested exceeds the energy threshold E_{th} right after the first time slot in the first phase and the primary signal x_p fails to be decoded by the PR in the second phase, by letting $x = |h_{p,s}(1)|^2$, $y = |h_{s,p}|^2$ and $z = |h_{p,p}|^2$, the corresponding probability $\Pr\{\mathcal{E}_{1,out}\}$ can be derived as

$$\begin{cases} e^{-\frac{d_{p,s}^v E_{th}}{\eta \lambda P_p}} - d_{p,s}^v e^{\frac{d_{p,p}^v}{P_p \xi_2} \left(\frac{\xi_1 \sigma^2}{P_p} - \frac{\gamma_{p,0} \sigma^2}{P_p} \right)} \int_{\frac{E_{th}}{\eta \lambda P_p}}^{\infty} I_1(x) dx, \\ \text{when } 0 < \alpha \leq \frac{\gamma_{p,0}}{1 + \gamma_{p,0}}, \\ e^{-\frac{d_{p,s}^v E_{th}}{\eta \lambda P_p}} - \Gamma \left(1, \frac{d_{p,s}^v E_{th}}{\eta \lambda P_p}; \frac{d_{p,s}^v d_{s,p}^v \gamma_{p,0} \sigma^2}{\phi_1} \right) \\ - d_{p,p}^v e^{\frac{d_{p,p}^v}{P_p \xi_2} \left(\frac{\xi_1 \sigma^2}{P_p} - \frac{\gamma_{p,0} \sigma^2}{P_p} \right)} \int_{\frac{E_{th}}{\eta \lambda P_p}}^{\infty} [I_1(x) - I_2(x)] dx, \\ \text{when } \frac{\gamma_{p,0}}{1 + \gamma_{p,0}} < \alpha < 1. \end{cases} \quad (28)$$

Proof: See Appendix C. ■

Lemma 2: For event $\mathcal{E}_{2,out}^{(t)}$ that the energy harvested exceeds the energy threshold E_{th} right after the t th time slot in the first phase and the primary signal x_p fails to be decoded by the PR in the second phase, by letting $x = \sum_{i=1}^{t-1} |h_{p,s}(i)|^2$, $y = |h_{p,s}(t)|^2$, $z = |h_{s,p}|^2$ and $w = \sum_{i=1}^t |h_{p,p}(i)|^2$, the corresponding probability $\Pr\{\mathcal{E}_{2,out}^{(t)}\}$ can be obtained as

$$\begin{cases} \int_0^{\frac{E_{th}}{\eta\lambda P_p}} \int_{\frac{E_{th}}{\eta\lambda P_p}-x}^{\infty} \int_0^{\infty} I(x, y, z) \\ \quad \times \gamma[t, d_{p,p}^v f(x, y, z)] dz dy dx, & 0 < \alpha \leq \frac{\gamma_{p,0}}{1+\gamma_{p,0}} \\ \int_0^{\frac{E_{th}}{\eta\lambda P_p}} \int_{\frac{E_{th}}{\eta\lambda P_p}-x}^{\infty} \int_0^{\frac{\gamma_{p,0}\sigma^2}{(x+y)\phi_1}} I(x, y, z) \\ \quad \times \gamma[t, d_{p,p}^v f(x, y, z)] dz dy dx, & \frac{\gamma_{p,0}}{1+\gamma_{p,0}} < \alpha < 1, \end{cases} \quad (29)$$

where $f(x, y, z) = \frac{\gamma_{p,0}\sigma^2}{P_p} - \frac{\xi_1\sigma^2(x+y)z}{P_p\xi_2(x+y)z+\sigma^2}$, $I(x, y, z) = \frac{x^{t-2} d_{p,s}^v d_{s,p}^v e^{-(d_{p,s}^v x + d_{p,s}^v y + d_{p,p}^v z)}}{(t-2)!(t-1)!}$ and $\gamma(\alpha, x) = \int_0^x e^{-t} t^{\alpha-1} dt$ is the incomplete gamma function [53, eq. (8.350)].

Proof: See Appendix D. ■

Lemma 3: For event $\mathcal{E}_{3,out}$ that an energy outage occurs in the first phase, the ST remains silent in the second phase, and the PR has to rely on the received signals from the direct channel across N time slots. From (26), the corresponding probability $\Pr\{\mathcal{E}_{3,out}\}$ can be derived as

$$\begin{aligned} \Pr\left\{x < \frac{E_{th}}{\eta\lambda P_p}, y < \frac{\gamma_{p,0}\sigma^2}{P_p}\right\} \\ &= \int_0^{\frac{E_{th}}{\eta\lambda P_p}} \frac{x^{N-1} d_{p,s}^v e^{-d_{p,s}^v x}}{(N-1)!} \\ &\quad \int_0^{\frac{\gamma_{p,0}\sigma^2}{P_p}} \frac{y^{N-1} d_{p,p}^v e^{-d_{p,p}^v y}}{(N-1)!} dy dx \\ &= \frac{\gamma\left(N, \frac{d_{p,s}^v E_{th}}{\eta\lambda P_p}\right) \gamma\left(N, \frac{d_{p,p}^v \gamma_{p,0}\sigma^2}{P_p}\right)}{(N-1)!(N-1)!}, \end{aligned} \quad (30)$$

by letting $x = \sum_{i=1}^N |h_{p,s}(i)|^2$ and $y = \sum_{i=1}^N |h_{p,p}(i)|^2$.

C. Outage Analysis of Secondary System

Theorem 4: For the proposed EAR scheme, taking into account of all possible events \mathcal{E}_1 , \mathcal{E}_2 and \mathcal{E}_3 in the first phase, the overall end-to-end outage probability of the secondary system can be similarly expressed as

$$\begin{aligned} O_s &= \Pr\left\{\underbrace{\mathcal{E}_1 \cap \left\{\gamma_s^{(1)} < \gamma_{s,0}\right\}}_{\mathcal{E}_{1,out}}\right\} \\ &\quad + \sum_{t=2}^N \Pr\left\{\underbrace{\mathcal{E}_2^{(t)} \cap \left\{\gamma_s^{(t)} < \gamma_{s,0}\right\}}_{\mathcal{E}_{2,out}^{(t)}}\right\} + \Pr\{\mathcal{E}_3\}. \end{aligned} \quad (31)$$

Proof: The probabilities $\Pr\{\mathcal{E}_{1,out}\}$, $\Pr\{\mathcal{E}_{2,out}^{(t)}\}$ and $\Pr\{\mathcal{E}_3\}$ are derived in *Lemma 4*, *Lemma 5* and *Lemma 6* respectively. ■

Lemma 4: For event $\mathcal{E}_{1,out}$ that assumes the energy harvested exceeds the energy threshold E_{th} right after the first time slot in the first phase and the secondary signal x_s fails to be decoded by the SR in the second phase, by letting $x = |h_{p,s}(1)|^2$ and $y = |h_{s,r}|^2$, the corresponding probability $\Pr\{\mathcal{E}_{1,out}\}$ can be derived as

$$\Pr\{\mathcal{E}_{1,out}\} = e^{-\frac{d_{p,s}^v E_{th}}{\eta\lambda P_p}} - \Gamma\left(1, \frac{d_{p,s}^v E_{th}}{\eta\lambda P_p}; \phi_2\right). \quad (32)$$

Proof: See Appendix E. ■

Lemma 5: For event $\mathcal{E}_{2,out}^{(t)}$ that the energy harvested exceeds the energy threshold E_{th} right after the t th time slot in the first phase and the secondary signal x_s fails to be decoded by the SR in the second phase, by letting $x = \sum_{i=1}^{t-1} |h_{p,s}(i)|^2$, $y = |h_{p,s}(t)|^2$ and $z = |h_{s,r}|^2$, we have the corresponding probability $\Pr\{\mathcal{E}_{2,out}^{(t)}\}$

$$\left(\frac{d_{p,s}^v E_{th}}{\eta\lambda P_p}\right)^{t-1} \left[e^{-\frac{d_{p,s}^v E_{th}}{\eta\lambda P_p}} - \Gamma\left(1, \frac{d_{p,s}^v E_{th}}{\eta\lambda P_p}; \phi_2\right) \right]. \quad (33)$$

Proof: See Appendix F. ■

Lemma 6: For event \mathcal{E}_3 that an energy outage occurs in the first phase, the ST remains silent and there is no way for the SR to recover x_s in the second phase. We have

$$\begin{aligned} \Pr\{\mathcal{E}_3\} &= \Pr\left\{x < \frac{E_{th}}{\eta\lambda P_p}\right\} \\ &= \int_0^{\frac{E_{th}}{\eta\lambda P_p}} \frac{x^{N-1} d_{p,s}^v e^{-d_{p,s}^v x}}{(N-1)!} dx \\ &= \frac{\gamma\left(N, \frac{d_{p,s}^v E_{th}}{\eta\lambda P_p}\right)}{(N-1)!}, \end{aligned} \quad (34)$$

by letting $x = \sum_{i=1}^N |h_{p,s}(i)|^2$.

D. Throughput Analysis

From Fig. 2(b), with normalization with respect to the number of time slots required to deliver a message, the average throughput (i.e., the total amount of data successfully delivered per time slot per Hz) can be similarly obtained. To be specific, conditioned on event \mathcal{E}_1 , it takes two time slots to deliver x_p and x_s to their respective destinations. Conditioned on event $\mathcal{E}_2^{(t)}$, where $t \in \{2, \dots, N\}$, it takes $(t+1)$ time slots to deliver x_p and x_s to their respective destinations. Conditioned on event \mathcal{E}_3 , an energy outage occurs and no relaying transmission is performed. Then, the SU experiences an outage and the PR attempts to decode x_p by using the signals received from the direct channel PT→PR. Thus, from (27) and (31), the average throughput achieved by the PU and the SU can

be respectively obtained as

$$T_p = \frac{(\Pr\{\mathcal{E}_1\} - \Pr\{\mathcal{E}_{1,out}\})R_p}{2} + \sum_{t=2}^N \frac{(\Pr\{\mathcal{E}_2^{(t)}\} - \Pr\{\mathcal{E}_{2,out}^{(t)}\})R_p}{t+1} + \frac{(\Pr\{\mathcal{E}_3\} - \Pr\{\mathcal{E}_{3,out}\})R_p}{N+1}, \quad (35)$$

$$T_s = \frac{(\Pr\{\mathcal{E}_1\} - \Pr\{\mathcal{E}_{1,out}\})R_s}{2} + \sum_{t=2}^N \frac{(\Pr\{\mathcal{E}_2^{(t)}\} - \Pr\{\mathcal{E}_{2,out}^{(t)}\})R_s}{t+1}. \quad (36)$$

V. SIMULATION RESULTS

In this section, simulation results are presented to demonstrate the performance of the proposed SWIPT-based cooperative spectrum sharing system under different schemes. Due to the inherent complexity of the considered system model and the proposed EAR scheme, our analytical expressions end up with some integrals that cannot be further simplified. However, it is worth noting that these integrals can be readily calculated by the integral tools in MATLAB. To reflect the relative locations of PT-PR and ST-SR while enabling operability of SWIPT, we let $d_{p,p} = 40\text{m}$, $d_{p,s} = 15\text{m}$, $d_{s,p} = 30\text{m}$, and $d_{s,r} = 30\text{m}$ for the direct channel PT→PR, relay channels PT→ST, ST→PR, and the secondary channel ST→SR [14], respectively. To reflect the relatively weak direct channel PT→PR, we adopt a greater path-loss exponent $\nu = 6$ for the direct channel PT→PR [44], [45] compared to the relay channels PT→ST→PR with $\nu = 3$ [14], [30]. For ease of illustration, we let the power splitting factor $\lambda = 0.2$, the power allocation factor $\alpha = 0.8$, the energy conversion efficiency $\eta = 0.8$, primary transmit power $P_p = 20\text{dBm}$, noise power $\sigma^2 = \sigma_0^2 = -80\text{dBm}$, the duration of a time slot equal to 1 second, target rates $R_p = R_s = 2\text{bits/s/Hz}$, retransmission threshold $N = 3$, and energy threshold for EH $E_{th} = -30\text{dBm(s)}$ respectively, unless otherwise specified. As shown in Fig. 3-Fig. 10, both the derived analytical results and Monte Carlo simulation results are presented, which are represented by lines and markers respectively.

Fig. 3 displays the impact of E_{th} and N on the outage performance of the PU. As shown in Fig. 3(a), O_p is plotted with respect to E_{th} when $N = 2, 3, 4$. With a very small $E_{th} = -40\text{dBm(s)}$ that can be easily met after the first transmission, the EAR scheme acts almost the same as the baseline scheme as if there is no constraint in the first phase, but suffers from performance loss due to limited energy available in the second phase. With an increase in E_{th} , since more energy can be potentially harvested by the ST, a better outage performance is achieved by the EAR scheme over the baseline scheme. With an unnecessarily high E_{th} , however, since the ST can hardly collect sufficient energy within a permitted number of retransmissions, the performance of the EAR scheme is severely degraded and becomes even worse than that of the baseline scheme. Thus, a proper E_{th} is required to strike a balance between the two successive phases, such

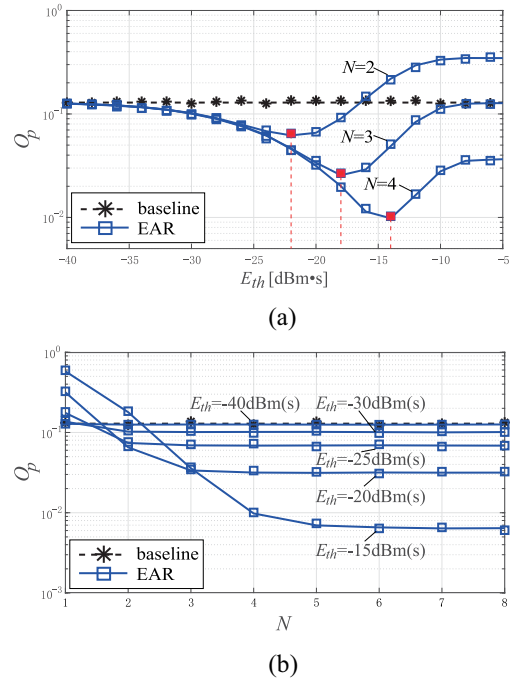


Fig. 3. The effects of E_{th} and N on the outage performance of PU. (a) O_p versus the energy threshold E_{th} for EH. (b) O_p versus the retransmission threshold N .

that a reasonably good end-to-end outage performance can be achieved.

Furthermore, with a higher N , in general it is beneficial to employ a larger E_{th} so that more energy can be harvested for achieving a better outage performance of the PU, as illustrated in Fig. 3(b). It is observed that a higher E_{th} generally requires a greater N in order to take full advantage of the EAR scheme, e.g., O_p under $E_{th} = -30\text{dBm(s)}$, -25dBm(s) , -20dBm(s) , -15dBm(s) becomes stable at about $N = 3, 4, 5, 7$, respectively. On the other hand, for a given N , while a small E_{th} leads to an under-utilization of the EAR scheme where more energy could have been harvested, an unnecessarily high E_{th} imposes an extra constraint on the first phase and could severely degrade the end-to-end outage performance. Thus, both E_{th} and N need to be properly selected¹ for exploiting the full potential of the proposed EAR scheme.

Fig. 4(a) demonstrates O_p versus R_p under different values of P_p . It is observed that the overall performance improves with a higher P_p and degrades with a greater R_p . Furthermore, with a small $E_{th} = -40\text{dBm(s)}$, both the EAR and baseline schemes have close performances, which agrees with the results shown in Fig. 3. On the other hand, with a greater $E_{th} = -30\text{dBm(s)}$, since more energy can be potentially harvested by the ST to power the relay transmission in the second phase, a better outage performance is achieved by the EAR scheme.

Fig. 4(b) demonstrates the system outage probability versus α . It is observed that a performance tradeoff exists between the PU and the SU in the proposed cooperative spectrum

¹In the rest of the simulations, a proper N is selected for a given E_{th} , according to the results illustrated in Fig. 3(b).

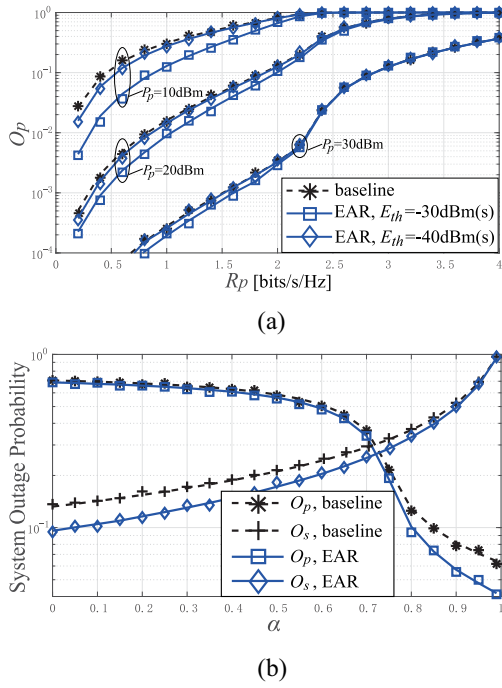


Fig. 4. The effects of R_p and α on the system outage performance. (a) O_p versus the primary target rate R_p . (b) O_p and O_s versus the power allocation factor α .

sharing system. This is because with a greater α , more energy is allocated to forward the primary signal at the ST, which ends up with a better performance of PU while degrading the performance of SU. It is also observed that both the PU and the SU under the EAR scheme outperform that under the baseline scheme under the prescribed parameter settings where $E_{th} = -30$ dBm(s) and $N = 3$.

Next we demonstrate the system average throughput in Fig. 5. From Fig. 5(a) where T_p is plotted with respect to R_p , we can observe that T_p after reaching its maximum value, decreases as R_p continues to increase. This is expected as T_p is limited by the low information rate and high outage probability in the low and high rate regions, respectively. In the low-rate region, the case without spectrum sharing outperforms the EAR and baseline schemes, which require at least two time slots to deliver a message. With an increase in R_p , the performance of the case without spectrum sharing suffers from a high outage probability, whereas a reasonably good outage performance can be maintained for the EAR and baseline schemes with the assistance of cooperative relaying. For the high rate scenario of $R_p = 3.6$ bits/s/Hz, the corresponding throughput T_p achieved by the baseline scheme and the EAR scheme with $E_{th} = -15$ dBm(s) is 0.0685 bits/s/Hz and 0.2936 bits/s/Hz respectively, which corresponds to a performance gain of 328.74% for the proposed EAR scheme. This is reasonable since almost no data can be reliably delivered by both the baseline scheme and the case without spectrum sharing due to very limited energy availability. At the same time, it is still possible for the proposed EAR scheme to successfully deliver some information by exploiting the energy harvested over retransmissions.

Similar phenomena can be observed in Fig. 5(b) where T_p is demonstrated versus P_p . It is observed that with an increase

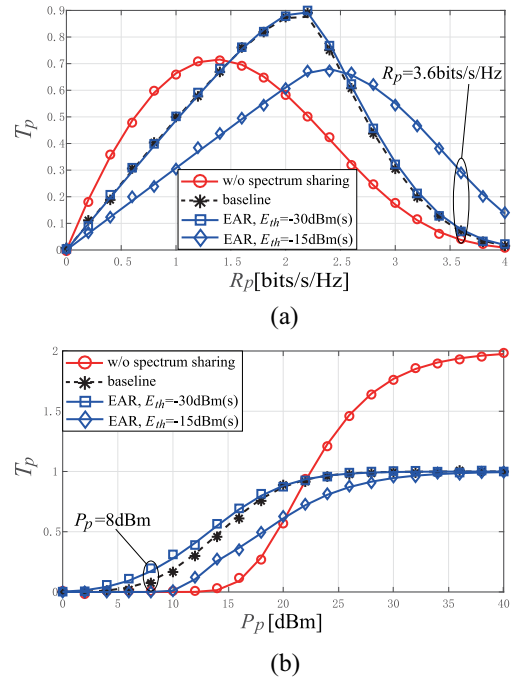


Fig. 5. The effects of different parameters on the average throughput of PU. (a) T_p versus primary target rate R_p . (b) T_p versus primary transmit power P_p .

of P_p , the overall throughput is enhanced and the case without spectrum sharing achieves a 2-fold throughput asymptotically compared to the EAR and baseline schemes that require at least two time slots for delivering a message. With a proper setting of $E_{th} = -30$ dBm(s), it can be observed that the EAR scheme performs the best in low-power regions. To be specific, when $P_p = 8$ dBm, the corresponding T_p achieved by the baseline and the proposed EAR schemes are 0.0909 bits/s/Hz and 0.1719 bits/s/Hz respectively. This indicates a performance gain of 89.11% for the proposed EAR scheme. However, with an unnecessarily high $E_{th} = -15$ dBm(s), since more time slots are required to meet E_{th} , the throughput of the EAR scheme is degraded and becomes even worse than the baseline scheme. From the observations in Fig. 5(a) and Fig. 5(b), the validity of the proposed EAR scheme is verified in unfavorable conditions due to *high-rate* and *low-power* requirements. It is worth noting that even under the non-linear EH model, the linearity holds in the low-power regime to a certain extent [15], [21]. It can then be expected that the performance gains achieved by the proposed EAR scheme in the low-power regime can still hold.

The system average throughput versus α is demonstrated in Fig. 6, where a performance tradeoff exists between the PU and the SU. By adopting $E_{th} = -30$ dBm(s) and $N = 3$, the EAR scheme achieves a slight performance improvement over the baseline scheme, as consistent with Fig. 5. Note that with a proper power allocation factor, specifically, $\alpha > 0.67$, a higher throughput of PU is achieved by the proposed cooperative spectrum sharing system than the system without spectrum sharing. Furthermore, the EAR scheme achieves a more than 2-fold sum throughput compared to the case without spectrum sharing at around $\alpha = 0.8$. This indicates that the system

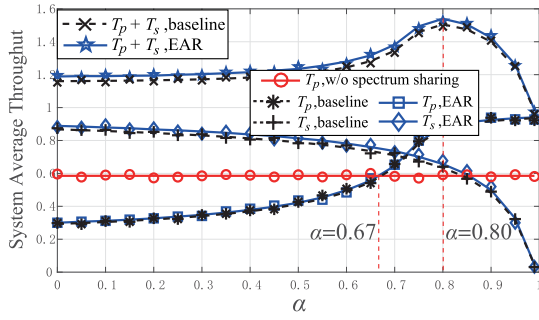


Fig. 6. System average throughput versus the power allocation factor α .

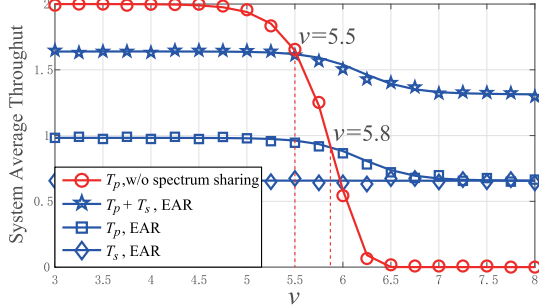


Fig. 7. System average throughput versus the path-loss exponent ν of the direct link $PT \rightarrow PR$.

spectrum efficiency can be significantly improved without consuming extra energy, thus building a win-win relationship between the PU and the SU.

In Fig. 7, the system average throughput is plotted with respect to the path-loss exponent ν of the direct link. With adjustable values of ν , the effect of path-loss attenuations can adapt to different environments covering free space to dense urban environmental conditions [44], [45]. It is observed that when $\nu = 3$, the case without spectrum sharing achieves an almost 2-fold throughput compared to the proposed EAR scheme. This is reasonable as direct transmission from PT to PR avoids spectrum efficiency loss due to the additional time slots required in the relay transmission. While the performance for the case without spectrum sharing is drastically deteriorated with an increase in ν , an acceptable performance can be maintained for the proposed EAR scheme. When $\nu > 5.5$, a higher sum throughput is achieved by the proposed EAR scheme. When $\nu > 5.8$, even the PU itself benefits from a performance gain under the proposed EAR scheme, let alone the throughput achieved by the SU. When $\nu > 6.5$, almost no data can be reliably delivered in the case without spectrum sharing, whereas a sum throughput of $T_p + T_s = 1.3$ bits/s/Hz can still be achieved under the proposed EAR scheme, owing to the relay transmission and the available energy at ST collected over retransmissions.

To reflect the impact of varying distances/locations of the nodes, we consider the network topology shown in Fig. 8(a). As can be seen, PT , PR , ST , SR are located at the original $(0, 0)$, $(d_{p,p}, 0)$, $(d_0, -5)$, $(d_0, -35)$, respectively and ST - SR moves along the X-axis where $d_0 \in (0, d_{p,p})$. Under these conditions, the average throughput T_p versus $\frac{d_0}{d_{p,p}}$ is plotted

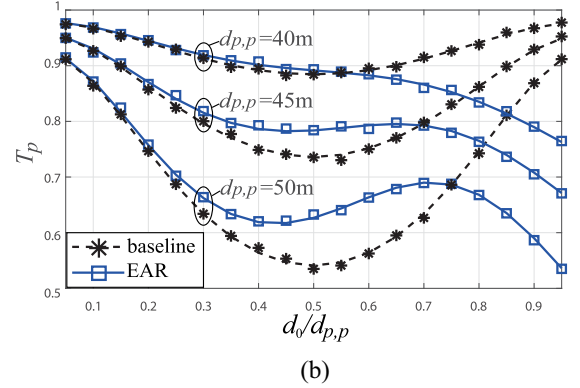
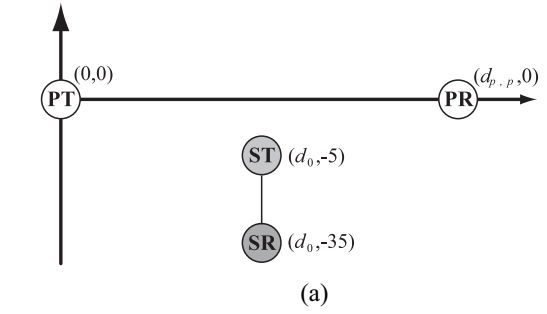


Fig. 8. An illustration of the impact of varying distances/locations of nodes on the system performance. (a) An illustration of the network topology. (b) T_p versus $d_0/d_{p,p}$ where $d_{p,p} = 40$ m, 45 m, 50 m.

in Fig. 8(b) under different distances $d_{p,p}$. We can clearly observe that with an increase in $d_{p,p}$, the overall throughput performance is degraded. Furthermore, for the baseline scheme in which the ST forwards the received signal with all energy available after a single transmission in the first phase, the throughput performance is symmetrical with respect to the location of the ST . This can be expected because when ST is located in the middle of PT and PR , the throughput performance suffers from limited harvested energy, as well as the worse relay channel $ST \rightarrow PR$. On the other hand, when ST is located very close to PT , similar performances can be achieved for both the baseline and the proposed EAR schemes. This is reasonable as the energy threshold E_{th} can readily be met right after the first transmission in the first phase. When ST moves away from PT , the relay channel condition: $PT \rightarrow ST$, worsens, hence severely limiting the energy availability at the ST in the case of the baseline scheme. At the same time, a better performance is achieved by the proposed EAR scheme owing to the energy accumulated over retransmissions. However, when ST keeps moving away from PT , since the relay channel $PT \rightarrow ST$ becomes so weak that the energy threshold E_{th} can be hardly met, the performance of the proposed EAR scheme is severely degraded and becomes even worse compared to the baseline scheme. Thus, in order to take full advantage of the proposed EAR scheme, the energy threshold E_{th} needs to be properly selected by taking into account the channel conditions (e.g., distances and locations of nodes).

Together with Fig. 4(a) and Fig. 5(a), T_p is drawn versus O_p in Fig. 9(a) under different values of R_p . We can observe that T_p and O_p cannot reach optimum values simultaneously.

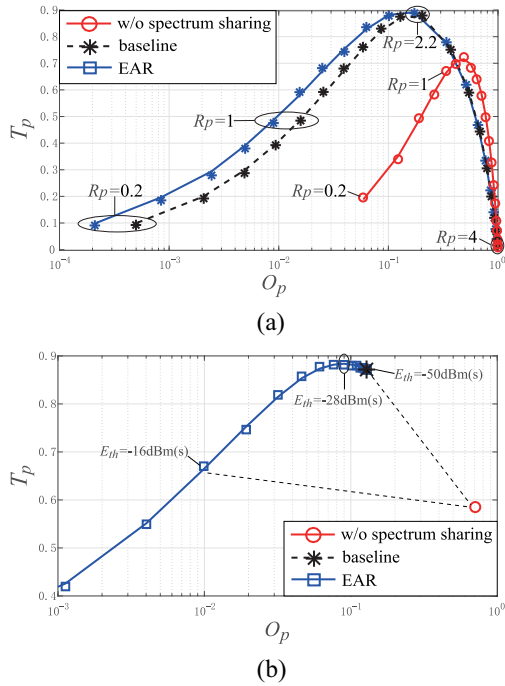


Fig. 9. An illustration of the performance tradeoff between T_p and O_p . (a) T_p versus O_p under different R_p . (b) T_p versus O_p under different E_{th} .

This tradeoff is based on a fact that in the low-outage region, T_p is limited by the low information rate. Whereas in the high-rate region, T_p is limited by the high outage probability, as consistent with Fig. 5(a). Under the same target rate, the EAR scheme performs the best in terms of outage probability. This, however, may not directly translate into throughput gain due to more occupied time slots, especially when an unnecessarily high E_{th} is adopted.

T_p is plotted with respect to O_p under different values of E_{th} in Fig. 9(b) when $R_p = 2$ bit/s/Hz. It is observed that while O_p keeps decreasing, the corresponding T_p after reaching the maximum value at around $E_{th} = -28$ dBm(s), decreases with an increase in E_{th} . This is reasonable as with a very small $E_{th} = -50$ dBm(s), it takes only two time slots to deliver a message as in the baseline scheme, but at the cost of a high outage probability. Conversely, with an unnecessarily high E_{th} , more energy can be harvested that enables a higher probability of successfully delivering the message, but at the cost of degraded throughput due to more time slots required. Furthermore, it is observed that when $E_{th} \leq -16$ dBm(s), the lines and markers of the EAR and baseline schemes always lie to the top left of the red circle, thus outperforming the system without spectrum sharing in terms of both outage and throughput.

To provide more insights, the system energy efficiency, defined as the successfully delivered information bits per joule, i.e., $\frac{T_p + T_s}{P_p}$, is plotted in Fig. 10 with respect to P_p . As can be seen when $E_{th} = -30$ dBm(s), the EAR scheme outperforms the baseline scheme in that the energy flow matches well with the information flow by exploiting the energy harvested over retransmissions potentially. Similarly, with an unnecessarily great $E_{th} = -15$ dBm(s), the performance of the EAR scheme is degraded and becomes worse than that of the

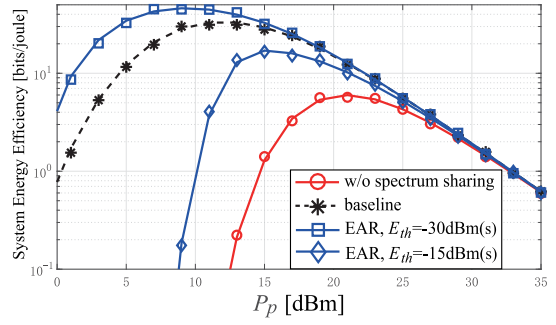


Fig. 10. System energy efficiency versus primary transmit power P_p .

baseline scheme. Furthermore, it is observed that significant performance gains are achieved by the proposed EAR and baseline schemes over the system without spectrum sharing, in both low and modest power regions.

VI. CONCLUSION

In this paper, a cooperative spectrum sharing system assisted by an SWIPT-based cognitive relay is considered. Based on a two-phase AF model, the cognitive relay attempts to forward a linearly weighted sum of the primary and secondary signals by using energy scavenged from the RF radiations of the PU. An EAR scheme is proposed for guaranteeing that a certain minimum amount of energy is harvested. The outage probability and average throughput are theoretically analyzed for both the PU and the SU under the proposed scheme. Simulation results demonstrate that a win-win situation is built between the PU and the SU with proper parameter settings. Furthermore, with an appropriate selection of thresholds for EH and retransmissions, additional performance gains can be achieved by the proposed EAR scheme in unfavorable conditions imposed by high rate and low power. As extensions of this work, a joint optimization of the energy threshold and the retransmission threshold can be conducted to adapt the energy flow to the information flow. Additionally, the initial energy available at the cognitive relay at the beginning of a message transmission can be taken into consideration, which is able to further improve the performance of the SWIPT-based cooperative spectrum sharing system.

APPENDIX A PROOF OF THEOREM 1

By letting $x = |h_{p,s}|^2$, $y = |h_{s,p}|^2$ and $z = |h_{p,p}|^2$, and substituting (6) into (8), we have

$$\begin{aligned}
 O_p &= \Pr \left\{ z < \frac{\gamma_{p,0}\sigma^2}{P_p} - \frac{\xi_1\sigma^2xy}{P_p\xi_2xy + \sigma^2} \right\} \\
 &= \Pr \left\{ P_p(\xi_1 - \xi_2\gamma_{p,0})xy < \gamma_{p,0}\sigma^2, \right. \\
 &\quad \left. z < \frac{\gamma_{p,0}\sigma^2}{P_p} - \frac{\xi_1\sigma^2xy}{P_p\xi_2xy + \sigma^2} \right\}. \quad (37)
 \end{aligned}$$

Since $x, y, z > 0$, we have the following two cases.

A. When $0 < \alpha \leq \frac{\gamma_{p,0}}{1+\gamma_{p,0}}$

In this case, we have $\xi_1 - \xi_2\gamma_{p,0} \leq 0$ and thus $P_p(\xi_1 - \xi_2\gamma_{p,0})xy \leq 0$. From (37), the corresponding outage probability can be rewritten as

$$\begin{aligned} & \Pr \left\{ z < \frac{\gamma_{p,0}\sigma^2}{P_p} - \frac{\xi_1\sigma^2xy}{P_p\xi_2xy + \sigma^2} \right\} \\ &= \int_0^\infty \int_0^\infty d_{p,s}^v d_{s,p}^v e^{-d_{p,s}^v x - d_{s,p}^v y} \\ & \quad \times \left[1 - e^{-d_{p,p}^v \left(\frac{\gamma_{p,0}\sigma^2}{P_p} - \frac{\xi_1\sigma^2xy}{P_p\xi_2xy + \sigma^2} \right)} \right] dy dx \\ &= 1 - d_{p,s}^v e^{d_{p,p}^v \left(\frac{\xi_1\sigma^2}{P_p\xi_2} - \frac{\gamma_{p,0}\sigma^2}{P_p} \right)} \int_0^\infty \\ & \quad \times e^{-d_{p,s}^v x + \frac{d_{s,p}^v\sigma^2}{P_p\xi_2x}} \Gamma \left(1, \frac{d_{s,p}^v\sigma^2}{P_p\xi_2x}; \frac{d_{s,p}^v\xi_1\sigma^4}{P_p^2\xi_2^2x} \right) dx, \quad (38) \end{aligned}$$

where $\Gamma(a, x; b)$ is the generalized incomplete Gamma function defined by $\Gamma(a, x; b) \triangleq \int_x^\infty t^{a-1} e^{-(t-\frac{b}{t})} dt$ [54].

For ease of expression, we let $I_1(x) = e^{-d_{p,s}^v x + \frac{d_{s,p}^v\sigma^2}{P_p\xi_2x}} \Gamma \left(1, \frac{d_{s,p}^v\sigma^2}{P_p\xi_2x}; \frac{d_{s,p}^v\xi_1\sigma^4}{P_p^2\xi_2^2x} \right)$.

B. When $\frac{\gamma_{p,0}}{1+\gamma_{p,0}} < \alpha < 1$

In this case, we have $P_p(\xi_1 - \xi_2\gamma_{p,0}) > 0$. Then by letting $\phi_1 = P_p(\xi_1 - \xi_2\gamma_{p,0})$, (37) can be rewritten as

$$\begin{aligned} & \Pr \left\{ x > 0, y < \frac{\gamma_{p,0}\sigma^2}{\phi_1 x}, z < \frac{\gamma_{p,0}\sigma^2}{P_p} - \frac{\xi_1\sigma^2xy}{P_p\xi_2xy + \sigma^2} \right\} \\ &= d_{p,s}^v d_{s,p}^v e^{-d_{p,s}^v x - d_{s,p}^v y} \\ & \quad \times \left[1 - e^{-d_{p,p}^v \left(\frac{\gamma_{p,0}\sigma^2}{P_p} - \frac{\xi_1\sigma^2xy}{P_p\xi_2xy + \sigma^2} \right)} \right] dy dx \\ &= 1 - 2\sqrt{\frac{d_{p,s}^v d_{s,p}^v \gamma_{p,0}\sigma^2}{\phi_1}} K_1 \left(2\sqrt{\frac{d_{p,s}^v d_{s,p}^v \gamma_{p,0}\sigma^2}{\phi_1}} \right) \\ & \quad - d_{p,s}^v e^{d_{p,p}^v \left(\frac{\xi_1\sigma^2}{P_p\xi_2} - \frac{\gamma_{p,0}\sigma^2}{P_p} \right)} \int_0^\infty [I_1(x) - I_2(x)] dx, \quad (39) \end{aligned}$$

where $K_\nu(\cdot)$ denotes the modified Bessel function of the second kind with order ν [53, eq. (3.324)], and $I_2(x) = e^{-d_{p,s}^v x + \frac{d_{s,p}^v\sigma^2}{P_p\xi_2x}} \Gamma \left(1, \frac{d_{s,p}^v\sigma^2}{P_p\xi_2x} + \frac{d_{p,p}^v\gamma_{p,0}\sigma^2}{\phi_1 x}; \frac{d_{s,p}^v\xi_1\sigma^4}{P_p^2\xi_2^2x} \right)$.

Together with the above two cases analyzed in (38) and (39), Theorem 1 is proved.

APPENDIX B PROOF OF THEOREM 2

By letting $x = |h_{p,s}|^2$ and $y = |h_{s,r}|^2$, and substituting (11) into (13), we have

$$O_s = \Pr \left\{ \frac{P_p\xi_2xy}{\sigma^2} < \gamma_{s,0} \right\} = \Pr \left\{ x > 0, y < \frac{\gamma_{s,0}\sigma^2}{P_p\xi_2x} \right\}$$

$$\begin{aligned} &= 1 - \int_0^\infty d_{p,s}^v e^{-d_{p,s}^v x} e^{-\frac{d_{s,r}^v\gamma_{s,0}\sigma^2}{P_p\xi_2x}} dx \\ &= 1 - 2\sqrt{\frac{d_{p,s}^v d_{s,r}^v \gamma_{s,0}\sigma^2}{P_p\xi_2}} K_1 \left(2\sqrt{\frac{d_{p,s}^v d_{s,r}^v \gamma_{s,0}\sigma^2}{P_p\xi_2}} \right) \\ &= 1 - 2\sqrt{\phi_2} K_1 \left(2\sqrt{\phi_2} \right), \quad (40) \end{aligned}$$

where $\phi_2 = \frac{d_{p,s}^v d_{s,r}^v \gamma_{s,0}\sigma^2}{P_p\xi_2}$.

Thus Theorem 2 is proved.

APPENDIX C PROOF OF LEMMA 1

By letting $x = |h_{p,s}(1)|^2$, $y = |h_{s,p}|^2$ and $z = |h_{p,p}|^2$, and substituting (22) into (27), the probability $\Pr\{\mathcal{E}_{1,out}\}$ can be expressed as

$$\begin{aligned} & \Pr \left\{ x \geq \frac{E_{th}}{\eta\lambda P_p}, \phi_1 xy < \gamma_{p,0}\sigma^2, \right. \\ & \quad \left. z < \frac{\gamma_{p,0}\sigma^2}{P_p} - \frac{\xi_1\sigma^2xy}{P_p\xi_2xy + \sigma^2} \right\}. \quad (41) \end{aligned}$$

Similar to the proof of Theorem 1 in Appendix A above we have the following two cases.

A. When $0 < \alpha \leq \frac{\gamma_{p,0}}{1+\gamma_{p,0}}$

In this case, we have $\phi_1 \leq 0$. Then (41) can be rewritten as

$$\begin{aligned} & \Pr \left\{ x \geq \frac{E_{th}}{\eta\lambda P_p}, z < \frac{\gamma_{p,0}\sigma^2}{P_p} - \frac{\xi_1\sigma^2xy}{P_p\xi_2xy + \sigma^2} \right\} \\ &= \int_{\frac{E_{th}}{\eta\lambda P_p}}^\infty \int_0^\infty d_{p,s}^v d_{s,p}^v e^{-d_{p,s}^v x - d_{s,p}^v y} \\ & \quad \times \left[1 - e^{-d_{p,p}^v \left(\frac{\gamma_{p,0}\sigma^2}{P_p} - \frac{\xi_1\sigma^2xy}{P_p\xi_2xy + \sigma^2} \right)} \right] dy dx \\ &= e^{-\frac{d_{p,s}^v E_{th}}{\eta\lambda P_p}} - d_{p,s}^v e^{d_{p,p}^v \left(\frac{\xi_1\sigma^2}{P_p\xi_2} - \frac{\gamma_{p,0}\sigma^2}{P_p} \right)} \int_{\frac{E_{th}}{\eta\lambda P_p}}^\infty I_1(x) dx. \quad (42) \end{aligned}$$

B. When $\frac{\gamma_{p,0}}{1+\gamma_{p,0}} < \alpha < 1$

In this case, we have $\phi_1 > 0$. From (41), similarly (41) can be rewritten as

$$\begin{aligned} & \Pr \left\{ x \geq \frac{E_{th}}{\eta\lambda P_p}, y < \frac{\gamma_{p,0}\sigma^2}{\phi_1 x}, \right. \\ & \quad \left. z < \frac{\gamma_{p,0}\sigma^2}{P_p} - \frac{\xi_1\sigma^2xy}{P_p\xi_2xy + \sigma^2} \right\} \\ &= e^{-\frac{d_{p,s}^v E_{th}}{\eta\lambda P_p}} - \Gamma \left(1, \frac{d_{p,s}^v E_{th}}{\eta\lambda P_p}; \frac{d_{p,s}^v d_{s,p}^v \gamma_{p,0}\sigma^2}{\phi_1} \right) \\ & \quad - d_{p,s}^v e^{d_{p,p}^v \left(\frac{\xi_1\sigma^2}{P_p\xi_2} - \frac{\gamma_{p,0}\sigma^2}{P_p} \right)} \int_{\frac{E_{th}}{\eta\lambda P_p}}^\infty [I_1(x) - I_2(x)] dx. \quad (43) \end{aligned}$$

Thus Lemma 1 is proved.

APPENDIX D
PROOF OF LEMMA 2

By letting $x = \sum_{i=1}^{t-1} |h_{p,s}(i)|^2$, $y = |h_{p,s}(t)|^2$, $z = |h_{s,p}|^2$ and $w = \sum_{i=1}^t |h_{p,p}(i)|^2$, and substituting (22) into (27), the probability $\Pr\{\mathcal{E}_{2,out}^{(t)}\}$ can be expressed as

$$\Pr\left\{x < \frac{E_{th}}{\eta\lambda P_p}, y \geq \frac{E_{th}}{\eta\lambda P_p} - x, \phi_1 z < \frac{\gamma_{p,0}\sigma^2}{x+y}, w < \frac{\gamma_{p,0}\sigma^2}{P_p} - \frac{\xi_1\sigma^2(x+y)z}{P_p\xi_2(x+y)z + \sigma^2}\right\}, \quad (44)$$

where $f(x, y, z) = \frac{\gamma_{p,0}\sigma^2}{P_p} - \frac{\xi_1\sigma^2(x+y)z}{P_p\xi_2(x+y)z + \sigma^2}$. Similar to the proof of Lemma 1 in Appendix C above, we have the following two cases.

A. When $0 < \alpha \leq \frac{\gamma_{p,0}}{1+\gamma_{p,0}}$

In this case, we have $\phi_1 \leq 0$, then (44) can be rewritten as

$$\begin{aligned} & \Pr\left\{x < \frac{E_{th}}{\eta\lambda P_p}, y \geq \frac{E_{th}}{\eta\lambda P_p} - x, w < f(x, y, z)\right\} \\ &= \int_0^{\frac{E_{th}}{\eta\lambda P_p}} \frac{x^{t-2} d_{p,s}^{v(t-1)} e^{-d_{p,s}^v x}}{(t-2)!} \int_{\frac{E_{th}}{\eta\lambda P_p} - x}^{\infty} d_{p,s}^v e^{-d_{p,s}^v y} \\ & \int_0^{\infty} d_{s,p}^v e^{-d_{s,p}^v z} \int_0^{\infty} \frac{f(x, y, z) w^{t-1} d_{p,p}^{vt} e^{-d_{p,p}^v w}}{(t-1)!} dw dz dy dx \\ &= \int_0^{\frac{E_{th}}{\eta\lambda P_p}} \int_{\frac{E_{th}}{\eta\lambda P_p} - x}^{\infty} \int_0^{\infty} \frac{x^{t-2} d_{p,s}^{vt} d_{s,p}^v}{(t-2)!(t-1)!} \\ & e^{-(d_{p,s}^v x + d_{s,p}^v y + d_{s,p}^v z)} \gamma[t, d_{p,p}^v f(x, y, z)] dz dy dx, \quad (45) \end{aligned}$$

where $\gamma(\alpha, x) = \int_0^x e^{-t} t^{\alpha-1} dt$ is the incomplete gamma function [53, eq. (8.350)].

For ease of expression, we let $I(x, y, z) = \frac{x^{t-2} d_{p,s}^{vt} d_{s,p}^v e^{-(d_{p,s}^v x + d_{s,p}^v y + d_{s,p}^v z)}}{(t-2)!(t-1)!}$. Here (45) is obtained by exploiting the property of the sum of a group of independent and identically distributed (i.i.d) random variables. To be specific, for a group of l i.i.d exponential random variables with a mean value ρ^{-1} , it has been proven that the sum of these random variables, denoted by z , follows a Gamma distribution with probability density function [61]

$$f_Z(z) = \begin{cases} \frac{z^{(l-1)} e^{-\rho z} \rho^l}{(l-1)!}, & z > 0 \\ 0, & \text{else.} \end{cases} \quad (46)$$

B. When $\frac{\gamma_{p,0}}{1+\gamma_{p,0}} < \alpha < 1$

In this case, we have $\phi_1 > 0$. Then from (44), similarly (44) can be rewritten as

$$\Pr\left\{x < \frac{E_{th}}{\eta\lambda P_p}, y > \frac{E_{th}}{\eta\lambda P_p} - x, z < \frac{\gamma_{p,0}\sigma^2}{(x+y)\phi_1}, w < f(x, y, z)\right\}$$

$$\begin{aligned} &= \int_0^{\frac{E_{th}}{\eta\lambda P_p}} \int_{\frac{E_{th}}{\eta\lambda P_p} - x}^{\infty} \int_0^{\frac{\gamma_{p,0}\sigma^2}{(x+y)\phi_1}} \\ & \times I(x, y, z) \gamma[t, d_{p,p}^v f(x, y, z)] dz dy dx. \quad (47) \end{aligned}$$

Thus Lemma 2 is proved.

APPENDIX E
PROOF OF LEMMA 4

By letting $x = |h_{p,s}(1)|^2$ and $y = |h_{s,r}|^2$, and substituting (24) into (31), the probability $\Pr\{\mathcal{E}_{1,out}\}$ can be expressed as

$$\begin{aligned} & \Pr\left\{x \geq \frac{E_{th}}{\eta\lambda P_p}, \frac{P_p \xi_2 xy}{\sigma^2} < \gamma_{s,0}\right\} \\ &= \Pr\left\{x \geq \frac{E_{th}}{\eta\lambda P_p}, y < \frac{\gamma_{s,0}\sigma^2}{P_p \xi_2 x}\right\} \\ &= e^{-\frac{d_{p,s}^v E_{th}}{\eta\lambda P_p}} - \int_{\frac{E_{th}}{\eta\lambda P_p}}^{\infty} d_{p,s}^v e^{-d_{p,s}^v x} e^{-\frac{d_{s,r}^v \gamma_{s,0}\sigma^2}{P_p \xi_2 x}} dx \\ &= e^{-\frac{d_{p,s}^v E_{th}}{\eta\lambda P_p}} - \Gamma\left(1, \frac{d_{p,s}^v E_{th}}{\eta\lambda P_p}; \phi_2\right). \quad (48) \end{aligned}$$

Thus Lemma 4 is proved.

APPENDIX F
PROOF OF LEMMA 5

By letting $x = \sum_{i=1}^{t-1} |h_{p,s}(i)|^2$, $y = |h_{p,s}(t)|^2$, $z = |h_{s,r}|^2$, and substituting (24) into (31), the probability of event $\mathcal{E}_{2,out}^{(t)}$ can be expressed as

$$\begin{aligned} & \Pr\left\{x < \frac{E_{th}}{\eta\lambda P_p}, y \geq \frac{E_{th}}{\eta\lambda P_p} - x, z < \frac{\gamma_{s,0}\sigma^2}{P_p \xi_2(x+y)}\right\} \\ &= \int_0^{\frac{E_{th}}{\eta\lambda P_p}} \frac{x^{t-2} d_{p,s}^{v(t-1)} e^{-d_{p,s}^v x}}{(t-2)!} \int_{\frac{E_{th}}{\eta\lambda P_p} - x}^{\infty} d_{p,s}^v e^{-d_{p,s}^v y} \\ & \times \left(1 - e^{-d_{s,r}^v \frac{\gamma_{s,0}\sigma^2}{P_p \xi_2(x+y)}}\right) dy dx \\ &= \frac{\left(\frac{d_{p,s}^v E_{th}}{\eta\lambda P_p}\right)^{t-1}}{(t-2)!(t-1)!} \left[e^{-\frac{d_{p,s}^v E_{th}}{\eta\lambda P_p}} - \Gamma\left(1, \frac{d_{p,s}^v E_{th}}{\eta\lambda P_p}; \phi_2\right)\right]. \quad (49) \end{aligned}$$

Thus Lemma 5 is proved.

REFERENCES

- [1] M.-L. Ku, W. Li, Y. Chen, and K. J. R. Liu, "Advances in energy harvesting communication: Past, present, and future challenges," *IEEE Commun. Surveys Tuts.*, vol. 18, no. 2, pp. 1384–1412, 2nd Quart., 2016.
- [2] S. Sudevalayam and P. Kulkarni, "Energy harvesting sensor nodes: Survey and implications," *IEEE Commun. Surveys Tuts.*, vol. 13, no. 3, pp. 443–461, 3rd Quart., 2011.
- [3] X. Lu, I. Flint, D. Niyato, N. Privault, and P. Wang, "Self-sustainable communications with RF energy harvesting: Gimibe point process modeling and analysis," *IEEE J. Sel. Areas Commun.*, vol. 34, no. 5, pp. 1518–1535, May 2016.
- [4] S. Kim *et al.*, "Ambient RF energy-harvesting technologies for self-sustainable standalone wireless sensor platforms," *Proc. IEEE*, vol. 102, no. 11, pp. 1649–1666, Nov. 2014.

- [5] K. Huang and V. K. N. Lau, "Enabling wireless power transfer in cellular networks: Architecture, modeling and deployment," *IEEE Trans. Wireless Commun.*, vol. 13, no. 2, pp. 902–912, Feb. 2014.
- [6] S. Bi, C. K. Ho, and R. Zhang, "Wireless powered communication: Opportunities and challenges," *IEEE Commun. Mag.*, vol. 53, no. 4, pp. 117–125, Apr. 2015.
- [7] K. Huang, C. Zhong, and G. Zhu, "Some new research trends in wirelessly powered communications," *IEEE Wireless Commun.*, vol. 23, no. 2, pp. 19–27, Apr. 2016.
- [8] Q. Li *et al.*, "Wireless-powered cooperative multi-relay systems with relay selection," *IEEE Access*, vol. 5, pp. 19058–19071, 2017.
- [9] A. A. Nasir, X. Zhou, S. Durrani, and R. A. Kennedy, "Relaying protocols for wireless energy harvesting and information processing," *IEEE Trans. Wireless Commun.*, vol. 12, no. 7, pp. 3622–3636, Jul. 2013.
- [10] X. Zhou, R. Zhang, and C. K. Ho, "Wireless information and power transfer: Architecture design and rate-energy tradeoff," *IEEE Trans. Wireless Commun.*, vol. 61, no. 11, pp. 4754–4767, Nov. 2013.
- [11] K. Huang and E. Larsson, "Simultaneous information and power transfer for broadband wireless system," *IEEE Trans. Signal Process.*, vol. 61, no. 23, pp. 5972–5985, Dec. 2013.
- [12] L. Liu, R. Zhang, and K.-C. Chua, "Wireless information and power transfer: A dynamic power splitting approach," *IEEE Trans. Wireless Commun.*, vol. 61, no. 9, pp. 3990–4001, Sep. 2013.
- [13] S. Lee and R. Zhang, "Cognitive wireless powered network: Spectrum sharing models and throughput maximization," *IEEE Trans. Cogn. Commun. Netw.*, vol. 1, no. 3, pp. 335–346, Sep. 2015.
- [14] Y. Ye *et al.*, "Optimal transmission schemes for DF relaying networks using SWIPT," *IEEE Trans. Veh. Technol.*, vol. 67, no. 8, pp. 7062–7071, Aug. 2018.
- [15] E. Boshkovska, D. W. K. Ng, N. Zlatanov, and R. Schober, "Practical non-linear energy harvesting model and resource allocation for SWIPT systems," *IEEE Commun. Lett.*, vol. 19, no. 12, pp. 2082–2085, Dec. 2015.
- [16] E. Boshkovska, R. Morsi, D. W. K. Ng, and R. Schober, "Power allocation and scheduling for SWIPT systems with non-linear energy harvesting model," in *Proc. IEEE ICC*, Kuala Lumpur, Malaysia, May 2016, pp. 1–6.
- [17] E. Boshkovska, D. W. K. Ng, N. Zlatanov, A. Koelpin, and R. Schober, "Robust resource allocation for MIMO wireless powered communication networks based on a non-linear EH model," *IEEE Trans. Commun.*, vol. 65, no. 5, pp. 1984–1999, May 2017.
- [18] S. Wang, M. Xia, K. Huang, and Y.-C. Wu, "Wirelessly powered two-way communication with nonlinear energy harvesting model: Rate regions under fixed and mobile relay," *IEEE Trans. Wireless Commun.*, vol. 16, no. 12, pp. 8190–8204, Dec. 2017.
- [19] Y. Huang, Z. Li, F. Zhou, and R. Zhu, "Robust AN-aided beamforming design for secure MISO cognitive radio based on a practical nonlinear EH model," *IEEE Access*, vol. 5, pp. 14011–14019, 2017.
- [20] Y. Wang, Y. Wang, F. Zhou, Y. Wu, and H. Zhou, "Resource allocation in wireless powered cognitive radio networks based on a practical nonlinear energy harvesting model," *IEEE Access*, vol. 5, pp. 17618–17626, 2017.
- [21] K. Xiong, B. Wang, and K. J. R. Liu, "Rate-energy region of SWIPT for MIMO broadcasting under nonlinear energy harvesting model," *IEEE Trans. Wireless Commun.*, vol. 16, no. 8, pp. 5147–5161, Aug. 2017.
- [22] G. Lu, L. Shi, and Y. Ye, "Maximum throughput of TS/PS scheme in an AF relaying network with non-linear energy harvester," *IEEE Access*, vol. 6, pp. 26617–26625, 2018.
- [23] A. Goldsmith, S. A. Jafar, I. Marić, and S. Srinivasa, "Breaking spectrum gridlock with cognitive radios: An information theoretic perspective," *Proc. IEEE*, vol. 97, no. 5, pp. 894–914, May 2009.
- [24] S. Park, H. Kim, and D. Hong, "Cognitive radio networks with energy harvesting," *IEEE Trans. Wireless Commun.*, vol. 12, no. 3, pp. 1386–1397, Mar. 2013.
- [25] S. Park and D. Hong, "Optimal spectrum access for energy harvesting cognitive radio networks," *IEEE Trans. Wireless Commun.*, vol. 12, no. 12, pp. 6166–6179, Dec. 2013.
- [26] D. T. Hoang, D. Niyato, P. Wang, and D. I. Kim, "Opportunistic channel access and RF energy harvesting in cognitive radio networks," *IEEE J. Sel. Areas Commun.*, vol. 32, no. 11, pp. 2039–2052, Nov. 2014.
- [27] S. Park and D. Hong, "Achievable throughput of energy harvesting cognitive radio networks," *IEEE Trans. Wireless Commun.*, vol. 13, no. 2, pp. 1010–1022, Feb. 2014.
- [28] S. Yin, Z. Qu, and S. Li, "Achievable throughput optimization in energy harvesting cognitive radio systems," *IEEE J. Sel. Areas Commun.*, vol. 33, no. 3, pp. 407–422, Mar. 2015.
- [29] Y. H. Bae and J. W. Baek, "Achievable throughput analysis of opportunistic spectrum access in cognitive radio networks with energy harvesting," *IEEE Trans. Commun.*, vol. 64, no. 4, pp. 1399–1410, Apr. 2016.
- [30] C. Zhai, J. Liu, and L. Zheng, "Relay-based spectrum sharing with secondary users powered by wireless energy harvesting," *IEEE Trans. Commun.*, vol. 64, no. 5, pp. 1875–1887, May 2016.
- [31] S. Lee, R. Zhang, and K. Huang, "Opportunistic wireless energy harvesting in cognitive radio networks," *IEEE Trans. Wireless Commun.*, vol. 12, no. 9, pp. 4788–4799, Sep. 2013.
- [32] Z. Yang, Z. Ding, P. Fan, and G. K. Karagiannidis, "Outage performance of cognitive relay networks with wireless information and power transfer," *IEEE Trans. Veh. Technol.*, vol. 65, no. 5, pp. 3828–3833, May 2016.
- [33] S. S. Kalamkar and A. Banerjee, "Interference-aided energy harvesting: Cognitive relaying with multiple primary transceivers," *IEEE Trans. Cogn. Commun. Netw.*, vol. 3, no. 3, pp. 313–327, Sep. 2017.
- [34] C. Zhai, J. Liu, and L. Zheng, "Cooperative spectrum sharing with wireless energy harvesting in cognitive radio networks," *IEEE Trans. Veh. Technol.*, vol. 65, no. 7, pp. 5303–5316, Jul. 2016.
- [35] O. Simeone *et al.*, "Spectrum leasing to cooperating secondary ad hoc networks," *IEEE J. Sel. Areas Commun.*, vol. 26, no. 1, pp. 203–213, Jan. 2008.
- [36] S. Yin, E. Zhang, Z. Qu, L. Yin, and S. Li, "Optimal cooperation strategy in cognitive radio systems with energy harvesting," *IEEE Trans. Wireless Commun.*, vol. 13, no. 9, pp. 4693–4707, Sep. 2014.
- [37] Z. Wang *et al.*, "Outage analysis of cognitive relay networks with energy harvesting and information transfer," in *Proc. IEEE Int. Conf. Commun. (ICC)*, Jun. 2014, pp. 4348–4353.
- [38] Z. Wang, Z. Chen, B. Xia, L. Luo, and J. Zhou, "Cognitive relay networks with energy harvesting and information transfer: Design, analysis, and optimization," *IEEE Trans. Wireless Commun.*, vol. 15, no. 4, pp. 2562–2576, Apr. 2016.
- [39] D. K. Verma, R. Y. Chang, and F.-T. Chien, "Energy-assisted decode-and-forward for energy harvesting cooperative cognitive networks," *IEEE Trans. Cogn. Commun. Netw.*, vol. 3, no. 3, pp. 328–342, Sep. 2017.
- [40] J. Yan and Y. Liu, "A dynamic SWIPT approach for cooperative cognitive radio networks," *IEEE Trans. Veh. Technol.*, vol. 66, no. 12, pp. 11122–11136, Dec. 2017.
- [41] Y. Wang, W. Lin, R. Sun, and Y. Huo, "Optimization of relay selection and ergodic capacity in cognitive radio sensor networks with wireless energy harvesting," *Pervasive Mobile Comput.*, vol. 22, pp. 33–45, Sep. 2015.
- [42] F. Benkhalifa and M.-S. Alouini, "Prioritizing data/energy thresholding-based antenna switching for SWIPT-enabled secondary receiver in cognitive radio networks," *IEEE Trans. Cogn. Commun. Netw.*, vol. 3, no. 4, pp. 782–800, Dec. 2017.
- [43] A. Banerjee, A. Paul, and S. P. Maity, "Joint power allocation and route selection for outage minimization in multihop cognitive radio networks with energy harvesting," *IEEE Trans. Cogn. Commun. Netw.*, vol. 4, no. 1, pp. 82–92, Mar. 2018.
- [44] Z. Ren, G. Wang, Q. Chen, and H. Li, "Modelling and simulation of Rayleigh fading, path loss, and shadowing fading for wireless mobile networks," *Simulat. Model. Pract. Theory*, vol. 19, no. 2, pp. 626–637, Feb. 2011.
- [45] N. I. Miridakis, T. A. Theodoros, G. C. Alexandropoulos, and M. Debbah, "Green cognitive relaying: Opportunistically switching between data transmission and energy harvesting," *IEEE J. Sel. Areas Commun.*, vol. 34, no. 12, pp. 3725–3738, Dec. 2016.
- [46] T. Kalluri, M. Peer, V. A. Bohara, D. B. Costa, and U. S. Dias, "Cooperative spectrum sharing-based relaying protocols with wireless energy harvesting cognitive user," *IET Commun.*, vol. 12, no. 7, pp. 838–847, Apr. 2018.
- [47] J. Zhan, Y. Liu, X. Tang, and Q. Chen, "Relaying protocols for buffer-aided energy harvesting wireless cooperative networks," *IET Netw.*, vol. 7, pp. 109–118, Jan. 2018.
- [48] Y. Han, A. Pandharipande, and S. H. Ting, "Cooperative decode-and-forward relaying for secondary spectrum access," *IEEE Trans. Wireless Commun.*, vol. 8, no. 10, pp. 4945–4950, Oct. 2009.
- [49] Q. Li, S. H. Ting, A. Pandharipande, and Y. Han, "Cognitive spectrum sharing with two-way relaying systems," *IEEE Trans. Veh. Technol.*, vol. 60, no. 3, pp. 1233–1240, Mar. 2011.
- [50] S. Lee, W. Su, S. Batalama, and J. D. Matyjias, "Cooperative decode-and-forward ARQ relaying: Performance analysis and power optimization," *IEEE Trans. Wireless Commun.*, vol. 9, no. 8, pp. 2632–2642, Aug. 2010.

- [51] B. Maham, A. Behnad, and M. Debbah, "Analysis of outage probability and throughput for half-duplex hybrid-ARQ relay channels," *IEEE Trans. Veh. Technol.*, vol. 61, no. 7, pp. 3061–3070, Sep. 2012.
- [52] T. Li, P. Fan, and K. B. Letaief, "Outage probability of energy harvesting relay-aided cooperative networks over Rayleigh fading channel," *IEEE Trans. Veh. Technol.*, vol. 65, no. 2, pp. 972–979, Feb. 2016.
- [53] I. S. Gradshteyn and I. M. Ryzhik, *Table of Integrals, Series, and Products*, 6th ed. New York, NY, USA: Academic, 2000.
- [54] Y. Gu and S. Aïssa, "RF-based energy harvesting in decoded-and-forward relaying system: Ergodic and outage capacities," *IEEE Trans. Wireless Commun.*, vol. 14, no. 11, pp. 6425–6435, Nov. 2015.
- [55] Y. Zhao *et al.*, "Wireless information and power transfer on cooperative multi-path relay channels," in *Proc. IEEE ICC*, 2016, pp. 1–6.
- [56] I. Krikidis, "Relay selection in wireless powered cooperative networks with energy storage," *IEEE J. Sel. Areas Commun.*, vol. 33, no. 12, pp. 2596–2610, Dec. 2015.
- [57] S. A. Mousavifar and C. Leung, "Lifetime analysis of a two-hop amplify-and-forward opportunistic wireless relay network," *IEEE Trans. Wireless Commun.*, vol. 12, no. 3, pp. 1186–1195, Mar. 2013.
- [58] Q. Li, S. H. Ting, A. Pandharipande, and M. Motani, "Cooperate-and-access spectrum sharing with ARQ-based primary systems," *IEEE Trans. Commun.*, vol. 60, no. 10, pp. 2861–2871, Oct. 2012.
- [59] F. Simjee and P. H. Chou, "Everlast: Long-life, supercapacitor-operated wireless sensor node," in *Proc. Int. Symp. Low Power Electron. Design*, 2006, pp. 197–202.
- [60] M. Kaus, J. Kowal, and D. U. Sauer, "Modelling the effects of charge redistribution during self-discharge of supercapacitors," *Electrochimica Acta*, vol. 55, no. 25, pp. 7516–7523, 2010.
- [61] P. E. Oguntunde, O. A. Odetunmbi, and A. O. Adejunmo, "On the sum of exponentially distributed random variables: A convolution approach," *Eur. J. Stat. Probab.*, vol. 1, no. 2, pp. 1–8, Dec. 2013.



Qiang Li (M'16) received the B.Eng. degree in communication engineering from the University of Electronic Science and Technology of China, Chengdu, China, in 2007, and the Ph.D. degree in electrical and electronic engineering from Nanyang Technological University, Singapore, in 2011. From 2011 to 2013, he was a Research Fellow with Nanyang Technological University. Since 2013, he has been an Associate Professor with the Huazhong University of Science and Technology, Wuhan, China. He was a Visiting Scholar with the University of Sheffield, Sheffield, U.K., in 2015, for three months. His current research interests include future broadband wireless networks, cooperative communications, cognitive radios and spectrum sharing, simultaneous wireless information and power transfer, software-defined networks, and edge caching.



Xueyan Zhang received the B.Eng. degree from Hunan University, Changsha, China, in 2017. She is currently pursuing the master's degree with the Huazhong University of Science and Technology, Wuhan, China. Her current research interests include energy harvesting, wireless power transfer, full-duplex techniques, and cooperative communications.



Ashish Pandharipande (S'97–AM'98–M'03–SM'08) received the M.S. degrees in electrical and computer engineering and mathematics, and the Ph.D. degree in electrical and computer engineering from the University of Iowa, Iowa City, in 2000, 2001, and 2002, respectively.

Since 2002, he has been a Post-Doctoral Researcher with the University of Florida, a Senior Researcher with the Samsung Advanced Institute of Technology, and a Senior Scientist with Philips Research. He has held visiting positions with AT&T Laboratories, NJ, USA, and the Department of Electrical Communication Engineering, Indian Institute of Science, Bengaluru, India. He is currently a Lead Research and Development Engineer with Signify (new company name of Philips Lighting), Eindhoven, The Netherlands. His research interests are at the intersection of sensing, networking and controls, and system applications in domains like smart lighting systems, energy monitoring and control, and cognitive spectrum sharing. He is currently an Associate Editor of the IEEE SIGNAL PROCESSING LETTERS and the IEEE SENSORS JOURNAL, an Associate Editor of the IEEE JOURNAL ON BIOMEDICAL HEALTH AND INFORMATICS, and a member of the International Advisory Board, Lighting Research and Technology.



Xiaohu Ge (M'09–SM'11) received the Ph.D. degree in communication and information engineering from the Huazhong University of Science and Technology (HUST), China, in 2003. He was a Researcher with Aju University, South Korea, and the Politecnico Di Torino, Italy, from 2004 to 2005. He has been with HUST since 2005, where he is currently a Full Professor with the School of Electronic Information and Communications. He is an Adjunct Professor with the Faculty of Engineering and Information Technology, University of Technology Sydney, Australia. He was a Visiting Researcher with Heriot-Watt University, Edinburgh, U.K., in 2010, for two months. He has published about 190 papers in refereed journals and conference proceedings and has been granted about 15 patents in China. His research interests are in the area of mobile communications, traffic modeling in wireless networks, green communications, and interference modeling in wireless communications. He was a recipient of the Best Paper Awards from IEEE Globecom 2010. He served as the General Chair for the 2015 IEEE International Conference on Green Computing and Communications. He serves as an Associate Editor for the IEEE WIRELESS COMMUNICATIONS and the IEEE TRANSACTIONS ON GREEN COMMUNICATIONS AND NETWORKING.



Hamid Gharavi (M'79–SM'90–F'92–LF'13) received the Ph.D. degree from Loughborough University, U.K., in 1980. He joined the Visual Communication Research Department, AT&T Bell Laboratories, Holmdel, NJ, USA, in 1982. He was then transferred to Bell Communications Research (Bellcore) after the AT&T-Bell divestiture, where he became a consultant on video technology and a Distinguished Member of Research Staff. In 1993, he joined Loughborough University as a Professor and the Chair of communication engineering.

Since 1998, he has been with the National Institute of Standards and Technology, U.S. Department of Commerce, Gaithersburg, MD, USA. He was a core member of Study Group XV (Specialist Group on Coding for Visual Telephony) of the International Communications Standardization Body CCITT (ITU-T). His research interests include smart grid, wireless multimedia, mobile communications and wireless systems, mobile ad hoc networks, and visual communications. He holds eight U.S. patents and has over 150 publications in the above areas. He was a recipient of the Charles Babbage Premium Award from the Institute of Electronics and Radio Engineering in 1986, the IEEE CAS Society Darlington Best Paper Award in 1989, and the Washington Academy of Science Distinguished Career in Science Award for 2017. He served as a Distinguished Lecturer of the IEEE Communication Society. He has been a Guest Editor for a number of special issues of the PROCEEDINGS OF THE IEEE, including *Smart Grid, Sensor Networks and Applications, Wireless Multimedia Communications, Advanced Automobile Technologies*, and *Grid Resilience*. He was a TPC Co-Chair for IEEE SmartGridComm in 2010 and 2012. He served as an Editorial Board Member for the PROCEEDINGS OF THE IEEE from 2003 to 2008. From 2010 to 2013, he served as the Editor-in-Chief for the IEEE TRANSACTIONS ON CIRCUITS AND SYSTEMS FOR VIDEO TECHNOLOGY. He is currently serving as the Editor-in-Chief for the IEEE WIRELESS COMMUNICATIONS.